Radio Science Bulletin

ISSN 1024-4530

INTERNATIONAL
UNION OF
RADIO SCIENCE

UNION
RADIO-SCIENTIFIQUE
INTERNATIONALE

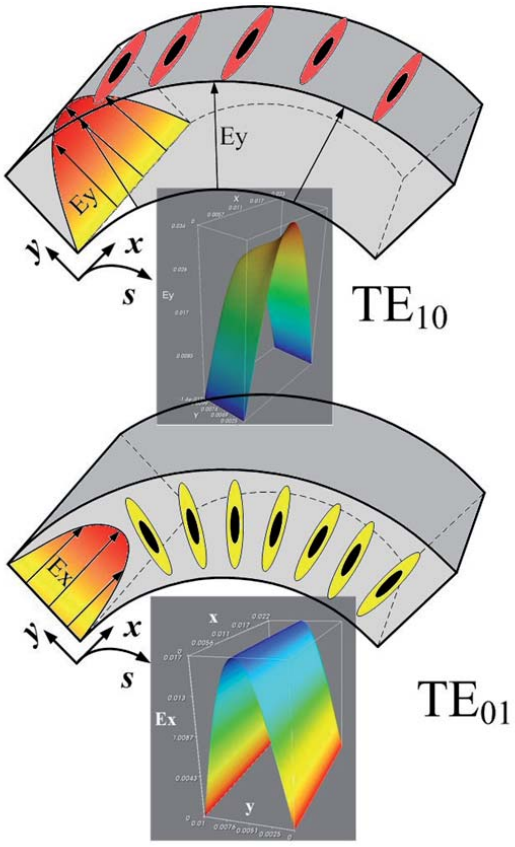

No 344
March 2013

URSI, c/o Ghent University (INTEC)
St.-Pietersnieuwstraat 41, B-9000 Gent (Belgium)

Contents

Editorial 3
Beijing GASS 4
In Memoriam 5
URSI Accounts 2012 7
IUCAF Annual Report for 2012 11
Eigenanalysis of Open Radiating, Periodic, and Curved Waveguide Structures 13
Radio-Frequency Radiation Safety and Health 32
Reassessing Exposure Safety Requirements for Mobile Phones 32
Wireless Battery-Charging Technology or Energy Harvesting to Power Mobile Phones or Other Mobile Communication Devices, and Health Effects 34
Book Reviews for Radioscientists 37
Conferences 40
MSMW'13 & TERATECH'13 45
AP-RASC'13 46
Information for authors 47

Front cover: The electric-field distributions for the TE_{10} *and* TE_{01} *modes in a curved section of WR-90 rectangular waveguide at 8.8 GHz. See the paper by G. A. Kyriacou, C. S. Lavranos, P. C. Allilomes, C. Zekios, S. Lavdas and A. V. Kudrin on pp. 13-31*

For information, please contact :
The URSI Secretariat
c/o Ghent University (INTEC)
Sint-Pietersnieuwstraat 41, B-9000 Gent, Belgium
Tel.: (32) 9-264 33 20, Fax: (32) 9-264 42 88
E-mail: info@ursi.org
http://www.ursi.org

Editorial

Our Featured Paper

In the invited paper in this issue, G. A. Kyriacou, C. S. Lavranos, P. C. Allilomes, C. Zekios, S. Lavdas and A. V. Kudrin describe the status and future directions of their work in analyzing waveguide structures. These include structures that are open or closed. They may be straight, curved, or periodic structures, and they may be loaded with anisotropic or inhomogeneous media. The authors begin with a review of the approaches that have been applied to this problem, pointing out the challenges. They then introduce two methods for the analysis: one is based on the Finite-Element Method, and the other is a finite-difference frequency-domain technique. A hybrid finite-element method for open waveguides is derived, and the approaches to handling some of the more-complicated structures are explained. A finite-difference frequency-domain method in orthogonal curvilinear coordinates is presented. A hybrid-domain finite-element and eigenfunction-expansion method for electrically large structures is derived, and its application to a reverberation chamber is explained. The use of the finite-difference frequency-domain method for the eigenanalysis of periodic waveguides is reviewed. Numerical results applying each of these methods to complex problems are presented. These results both demonstrate the computational efficiency of the authors' methods, and provide comparisons with results for the same structures obtained using other methods, to demonstrate the accuracy of the techniques. This is a fascinating review of a large body of work dealing with the electromagnetic analysis of an important class of problems, having direct application to real-world devices.

The efforts of Bill Davis, Yasuhiro Koyama, and P. Banerjee in bringing us this paper are gratefully acknowledged.

Our Other Contributions

Jim Lin has provided us with two contributions in his Radio-Frequency Radiation Safety and Health column. The first contribution looks at the possible implications and consequences resulting from a very recent report of the US Government Accountability Office (GAO) on mobile-phone safety. This report recommends that the US Federal Communications Commission reassess and, if appropriate, change its current RF exposure safety rules. The second contribution looks at the developing field of wireless charging for mobile devices. In addition to a review of what is being done in this field, the possible implications for public health and safety are considered.

Kristian Schlegel has provided us with two book reviews. One is from a Young Scientist, and both cover books of current interest to radio scientists.

We have a report on the fifth Workshop on VLF/ELF Remote Sensing of the Ionosphere and Magnetosphere (VERSIM). The calls for papers for conferences of interest to radio scientists also appear in this issue. Martin Hall made significant contributions to the remote sensing of rain, and to the understanding and modeling of its effects on radiowave propagation. He also was a very active supporter of URSI. He is remembered in an "In Memoriam" in this issue.

An Opportunity

The *Radio Science Bulletin* goes directly to those most active in the field of radio science. We are able to offer a very rapid way to get papers of broader interest in this field to those who are likely to be most interested in reading them. I urge you to contact me if you have a paper that you would like to get published.

Beijing GASS
16-23 August 2014

The XXXI General Assembly of the International Union of Radio Science will be held at the China National Convention Center (CNCC) in downtown Beijing, China on August 14-23, 2014. The General Assemblies of URSI are held at intervals of three years to review current research trends, present new discoveries and make plans for future research and special projects in all areas of radio science, especially where international cooperation is desirable. The first Assembly was held in Brussels, Belgium in 1922 and it is the first time the Assembly be held in Beijing, China.

As the host city of 2014 URSI GASS, Beijing is an ancient city with a long history. Back in 3000 years ago in Zhou dynasty, Beijing, which was called Ji at the moment, had been named capital of Yan. Thereafter, Liao, Jin, Yuan, Ming and Qing dynasties all made Beijing their capitals. Therefore, Beijing was famous for "Capital of a thousand years". The long history leaves Beijing precious cultural treasure. There are 7300 cultural relics and historic sites and more than 200 scenic spots -- including the world's largest palace, the Forbidden City, as well as the Great Wall, the only man-made structure that could been seen in the space; Summer Palace, a classic composition of ancient royal gardens, and Temple of Heaven, where the emperor used to fete their ancestors, and also the soul of Chinese ancient constructions. The four sites above-mentioned have been confirmed world cultural heritage by UNESCO.For the Olympics 2008 had been hold in Beijing , the spirit of "green Olympics, scientific Olympics and humanized Olympic" surely bring more and more changes to Beijing, and strengthen the friendly communications between Chinese and foreign people.

As the organizer of the Assembly, the Chinese Institute of Electronics (CIE), one department of the China Association for Science and Technology, is the largest national academic society in the electronic field in China. CIE has got great support from both the Chinese government and Chinese academic organizations, the State Council of People's Republic of China, Ministry of Science, National Natural Science Foundation of China and Technology and China Association for Science and Technology.

We have confidence to make the event to be the greatest one in its history. We sincerely invite every scientist of URSI community to attend the 2014 URSI General Assembly and Scientific Symposium in Beijing. More details on the URSI GASS 2014 website will be announced later.

We look forward to seeing you in Beijing in 2014.

CIE Committee for URSI

In Memoriam

Martin Hall
1937 - 2012

Martin Peter Maurice Hall, known as Martin to his professional colleagues and as Peter to his family, died on October 27, 2012. He had been combating cancer since 2010, but his health deteriorated rapidly in the middle of October 2012.

Martin spent much of his career at the Radio Research Station, Slough, which later became the Rutherford Appleton Laboratory. The RAL Chilbolton radar, intended for research on radiowave propagation and atmospheric physics, became operational in 1967. This pioneering radar operated in S band, and has a 25 m steerable-dish antenna. Martin recognized that radar could be used to investigate rain and other precipitation for its effects on radiowave propagation for terrestrial and Earth-space communications. The challenge was to improve the technique beyond simply measuring the strength of the echoes from rain, as had been done for some decades. Here, Martin's strength as a communicator was key, in that an almost chance meeting with T. A. Seliga and V. N. Bringi (at that time, with Ohio State University) led to a collaborative project that investigated and implemented dual-polarization radar. The modification for dual polarization at Chilbolton started in about 1978. It required a substantial redesign of the radar, including the feed system and the receiver/data processing. An essential part was the polarization switch, which enabled alternately transmitted pulses to be horizontally and vertically polarized. The fast polarization switching was the novel feature that enabled the two polarizations to be measured within a few milliseconds, and made possible measurement of the ratio of the reflectivity at the two polarizations to a few tenths of a dB. Otherwise, the noise-like nature of the echoes from rain would limit the accuracy to a few dB. The engineering implementation was due to Steve Cherry. Martin made the whole thing possible by bringing the people together and getting the support from RAL management and from the Science Research Council/Science and Engineering Research Council to fund the work. The other side of the work was to effectively present the results, and Martin was very good at this.

The first results were presented in a paper, "Rain Drop Sizes and Rainfall Rate Measured by Dual-Polarization Radar," in *Nature* in May 1980. This showed the ability to obtain two-dimensional spatial distributions of the statistical characteristics of the sizes and concentration of raindrops in rain, and to give a clear distinction between ice particles and raindrops. The data were used to estimate rainfall rates within small volumes to a much greater accuracy than was available from the conventional radar measurements being obtained at that time.

Martin was central to organizing an URSI Commission F symposium on multiple-parameter radar measurements of precipitation in 1982. The proceedings of that symposium detailed the principles of multi-parameter radar, and continue to be used as a reference.

Martin led the group at RAL that continued to develop the technique, providing invaluable models of rain events, of the melting layer in the troposphere, and the parameterization of climatic effects (radio refractivity and precipitation) on tropospheric propagation. This in turn was used in the development of propagation-prediction methods for the performance of terrestrial and Earth-space radio paths.

He was very active within the propagation study group of the International Radio Consultative Committee (CCIR), later the propagation study group of the Radiocommunication Sector of the International Telecommunication Union (ITU-R). Here, as Chair of the permanent Working Party 3M, he demonstrated his organizational ability with copious lists, notes, and future work programs, all aimed at driving the work forward, together with his interpersonal skills. As a part of this he also organized social events for the group. Whenever the group met away from Geneva, he arranged for a group tee shirt to be designed, produced, and distributed.

He was always keen to forge links between URSI and ITU-R, recognizing the potential value of radio science to the spectrum-engineering community. To this end, he made untiring efforts to bring together radio scientists and spectrum engineers from all over the world to share their knowledge and expertise. To support these mutual studies, a series of international meetings (known as CLIMPARA or CLIMDIFF) was held, linked in place and time with meetings of ITU-R Work Parties to allow the possibility of joint participation by the scientists and engineers concerned. Similar initiatives to link radio science with ongoing study topics in ITU-R were also made in remote sensing and spectrum management.

Martin was Vice Chair of URSI Commission F during 1993-1996, and Chair during 1996-1999. He was Assistant Coordinator of the Scientific Program for the Toronto General Assembly in 1999, and was Coordinator of the Scientific Program for the Maastricht General Assembly in 2002. As Chair of the URSI Scientific Committee on Telecommunications during 2002-2005, he sought to revive the initiatives to increase the cooperation and joint involvement between ITU-R Study Groups and URSI Commissions.

Martin Hall made great contributions to the advancement of radio science, particularly to the understanding of radiowave propagation. He will be remembered in the ITU-R Recommendations and in his published papers, and by those who had the good fortune to work with him. His family life was immensely important to him: he leaves his wife, Carol; two children, James and Susie; and four grandchildren, Rosie, Anna, Theo, and George.

Les Barclay
E-mail: les@lbarclay.demon.co.uk

URSI Accounts 2012

In a year following an URSI General Assembly and Scientific Symposium, the expenses are traditionally lower than other years in the URSI triennial cycle. This has also been the case for 2012 and thanks to the careful financial management by the URSI Board and control on the administrative expenses at the URSI Secretariat, the financial situation of URSI is still in good shape. Prudent and conservative management has resulted in safeguarding of the URSI reserves in the current difficult financial circumstances. This situation allows the continuation of some initiatives taken by the URSI Board during the previous years on stimulating the participation of Young Scientists in the URSI Community and increasing the visibility and the services of URSI in the scientific community.

URSI is however a scientific organization with long-term objectives in a world dominated by short term economical goals and continued care should be taken to keep the financial balance of our organization in control. Thanks to the continued effort and commitment of our URSI Communities and in spite of the economic crises which many of us experience, most of our Member Committees can still maintain their membership fees, which are the main basis of the income on which URSI operates. To ensure these contributions, URSI should continue to invest in young researchers, in new territories and team up with other organisations within and outside ICSU.

Prof. Paul Lagasse
Secretary General of URSI

BALANCE SHEET: 31 DECEMBER 2012

	EURO	EURO
ASSETS		
Dollars		
Merrill Lynch WCMA	0.00	
PNB Paribas Fortis	0.00	
Smith Barney Shearson	0.00	
		0.00
Euros		
Banque Degroof	152.08	
BNP Paribas Fortis zichtrekening	91,154.99	
BNP Paribas Fortis spaarrekening	155,180.02	
BNP Paribas Fortis portefeuillerekening	363,784.22	
		610,271.31
Investments		
Demeter Sicav Shares	22,681.79	
Rorento Units	111,614.53	
Aqua Sicav	63,785.56	
Bonds	104,000.00	
Merrill-Lynch Low Duration (304 units)	0.00	
Massachusetts Investor Fund	0.00	
Provision for (not realised) less value	0.00	
Provision for (not realised) currency differences	0.00	
	302,081.88	
673 Rorento units on behalf of van der Pol Fund	12,214.69	
		314,296.57
Petty Cash		63.23
Total Assets		924,631.11
Less Creditors		
IUCAF	22,257.84	
ISES	5,901.31	
		(28,159.15)
Balthasar van der Pol Medal Fund		(12,214.69)
NET TOTAL OF URSI ASSETS		**884,257.27**

The net URSI Assets are represented by:	EURO	EURO
Closure of Secretariat		
Provision for Closure of Secretariat		100,000.00
Scientific Activities Fund		
Scientific Activities in 2013	55,000.00	
Routine Meetings in 2013	15,000.00	
Publications/website in 2013	15,000.00	
Young Scientists in 2013	0.00	
Administration Fund in 2013	105,000.00	
I.C.S.U. Dues in 2013	10,000.00	
		200,000.00
XXXI GASS 2012/2014 Fund:		
During 2009-2010-2011 (GASS 2011)		0.00
During 2012-2013-2014 (GASS 2014)		100,000.00
Total allocated URSI Assets		300,000.00
Unallocated Reserve Fund		584,257.27
		884,257.27

Statement of Income and expenditure for the year ended 31 December 2012

I. INCOME		
Grant from ICSU Fund and US National Academy of Sciences	0.00	
Allocation from UNESCO to ISCU Grants Programme	0.00	
UNESCO Contracts	0.00	
Contributions from National Members (year -1)	4,060.00	
Contributions from National Members (year)	142,088.00	
Contributions from National Members (year +1)	37,552.00	
Contributions from Other Members	0.00	
Special Contributions	0.00	
Contracts	0.00	
Sales of Publications, Royalties	160.00	
Sales of scientfic materials	0.00	
Bank Interest	3,863.80	
Other Income	6,690.70	
Total Income		**194,414.50**
II. EXPENDITURE		
A1) Scientific Activities		65,691.57
General Assembly 2008/2011/2014	24,611.00	
Scientific meetings: symposia/colloqiua	7,870.75	
Working groups/Training courses	0.00	
Representation at scientific meetings	16,495.82	
Data Gather/Processing	0.00	
Research Projects	0.00	
Grants to Individuals/Organisations	0.00	
Other	16,714.00	
Loss covered by UNESCO Contracts	0.00	
A2) Routine Meetings		14,569.92
Bureau/Executive committee	14,569.92	
Other	0.00	

A3) Publications			3,345.71
B) Other Activities			9,296.00
Contribution to ICSU		7,296.00	
Contribution to other ICSU bodies		2,000.00	
Activities covered by UNESCO Contracts		0.00	
C) Administrative Expenses			98,211.35
Salaries, Related Charges		88,668.31	
General Office Expenses		2,881.88	
Travel and representation		1,003.84	
Office Equipment		3,548.13	
Accountancy/Audit Fees		5,469.20	
Bank Charges/Taxes		5,640.65	
Loss on Investments (realised/unrealised)		(9,000.66)	
Total Expenditure:			**191,114.55**
Excess of Expenditure over Income			3,299.95
Currency translation diff. (USD => EURO) - Bank Accounts			0.00
Currency translation diff. (USD => EURO) - Investments			0.00
Currency translation diff. (USD => EURO) - Others			0.00
Accumulated Balance at 1 January 2012			880,957.32
			884,257.27

Rates of exchange

January 1, 2012	1 $ = 0.7630 EUR
December 31, 2012	1 $ = 0.7540 EUR

Balthasar van der Pol Fund

673 Rorento Shares : market value on December 31 (Aquisition Value: USD 12.476,17/EUR 12.414,34)	36,570.82
Book Value on December 31, 2012/2011/2010/2009	12,214.69

Market Value of investments on December 31, 2012-2009

Demeter Sicav	78,780.90
Rorento Units (1)	706,420.00
Aqua-Sicav	89,919.95
M-L Low Duration	0.00
Massachusetts Investor Fund	0.00
Bonds	109,627.14
	984,747.99
Book Value on December 31, 2012/2011/2010/2009	314,296.57

(1) Including the 673 Rorento Shares of v d Pol Fund

APPENDIX : Detail of Income and Expenditure

I. INCOME		
Other Income		
Income General Assembly 2008	0.00	
Income General Assembly 2011	6,380.00	
Young scientist support (Japan)	0.00	
Support Koga Medal	0.00	
Closure Radio Science Press	0.00	
Commission B+C	0.00	
Income bonds	260.70	
Other	50.00	
		6,690.70
II . EXPENDITURE		
General Assembly 2008		
Organisation	0.00	
Vanderpol Medal	0.00	
Young scientists	0.00	
Expenses officials	0.00	
Support Commissions	0.00	
General Assembly 2011		
Organisation	23,561.12	
Vanderpol Medal	0.00	
Young scientists	0.00	
Expenses officials	914.53	
Support Commissions	0.00	
General Assembly 2014		
Organisation	135.35	
		24,611.00
Symposia/Colloquia/Working Groups		
Commission A	0.00	
Commission B	0.00	
Commission C	2,500.00	
Commission D	0.00	
Commission E	520.75	
Commission F	1,500.00	
Commission G	500.00	
Commission H	1,500.00	
Commission J	0.00	
Commission K	0.00	
Central Fund	0.00	
Central Fund (Student Award MC)	1,350.00	
		7,870.75
Contribution to other ICSU bodies		
FAGS	0.00	
IUCAF	2,000.00	
		2,000.00
Publications		
Printing ‘The Radio Science Bulletin’	1,570.51	
Mailing ‘The Radio Science Bulletin’	1,775.20	
		3,345.71

IUCAF Annual Report for 2012

1. Introduction

The Scientific Committee on Frequency Allocations for Radio Astronomy and Space Science, IUCAF, was formed in 1960 by its sponsoring Scientific Unions, URSI, the IAU, and COSPAR. Its brief is to study and coordinate the requirements of radio frequency allocations for passive (i.e., non-emitting or receive-only) radio sciences, such as radio astronomy, space research and remote sensing, in order to make these requirements known to the national administrations and international bodies that allocate frequencies. IUCAF operates as a standing inter-disciplinary committee under the auspices of ICSU, the International Council for Science. IUCAF is a Sector Member of the International Telecommunication Union (ITU).

2. Membership

At the end of 2012 the membership for IUCAF was:

URSI	S. Ananthakrishnan (Com J)	India
	S. Reising (Com F)	USA
	I. Häggström (Com G)	Sweden
	A. Tzioumis (Com J)	Australia
	W. van Driel (Com J)	France
IAU	H. Chung	rep. of Korea
	H.S. Liszt (Vice Chair)	USA
	M. Ohishi (Chair)	Japan
	T. Gergely	USA
	A. Tiplady	South Africa
	Y. Murata	Japan
at large:	W.A. Baan	the Netherlands
	D.T. Emerson	USA

IUCAF also has a group of Correspondents, in order to improve its global geographic representation and for issues on spectrum regulation concerning astronomical observations in the optical and infrared domains. At the General Assembly of the IAU, held in Beijing, China, in August 2012, Dr. Tomas Gergely (USA) was appointed an IUCAF member to be replaced with Dr. K.F. Tapping. IUCAF expresses its best appreciation to Dr. K.F. Tapping (Canada) who served as a very active IUCAF member for a long time. All IUCAF members wish Dr. Tapping's happy retirement life.

3. International Meetings

During the period of January to December 2012, its Members and Correspondents represented IUCAF in the following international meetings:

January-February	World Radiocommunication Conference 2012 (WRC-2012) Geneva, Switzerland
May	ITU-R Study Group 7 (Science services) Geneva, Switzerland
June	Space Frequency Coordination Group meeting (SFCG-32) Darmstadt, Germany
August	IAU General Assembly Beijing, China
September	ITU Special Seminar on Spectrum Management, and Working Party 7D (Radio Astronomy) Manta, Ecuador

Additionally, many IUCAF members and its associates participated in numerous national or regional meetings (including CORF, CRAF, RAFCAP, the FCC etc.), dealing with spectrum management issues, such as the preparation of input documents to various ITU meetings.

4. IUCAF Business Meetings

During 2012 IUCAF had face-to-face committee meetings. Before and during the WP7D meeting IUCAF ad-hoc meetings were held to discuss further its meeting strategy.

In the business meeting during the IAU GA, financial issues, approval of the new member, review of the "Terms of Reference", initiatives and future contributions to international spectrum management meetings and so on were discussed. Dr. Tomas Gergely (USA) was appointed an IUCAF member to be replaced with Dr. K.F. Tapping. Since the "ToR" is over 40 years old, revision of the "ToR" would be required soon.

Although such face-to-face meetings have been convenient and effective, throughout the year much IUCAF business is undertaken via e-mail communications between the members and correspondents.

5. Protecting the Passive Radio Science Services

The most important event in protecting the passive radio science services occurred during the World Radiocommunication Conference in 2012 (WRC-12) of the ITU, which was held between January and February, 2012, in Geneva, Switzerland. WRCs are held in every 3-4 years

for updating international rules (the Radio Regulations) in using the frequency resource, which will then be referred to by each government in order to update its national radio act.

The frequency range between 275 and 3000 GHz is used by the passive radio science observations of many spectral lines and continuum bands. These observations assist in astronomical studies and understanding of the Universe as well as passive satellite observations by the Earth science community.

Although no frequency allocations have been made above 275 GHz, the radio astronomy community and the Earth science community have identified a list of specific bands of interest which need to be protected by each government. Thus a WRC-12 agenda item to review the use of the radio spectrum between 275 and 3000 GHz was most relevant to the passive radio science concerns. Fortunately an agreement was made towards updating a footnote (5.565) in the Radio Regulations of the ITU at the WRC 2012, resulting in better protection of passive radio sciences between 275 and 3000 GHz. The new international regulatory measure has been in effect from 2013 on.

A WRC is a venue to approve future agenda items. The next WRC is scheduled to be held in 2015 (WRC-15); an agenda item regarding the protection of radio astronomical observations from possible (highly probable) interference caused by collision avoidance radars at around 79 GHz region is of importance to the radio astronomy community. Relevant technical discussion has been going on since the September 2012 meeting of WP 7D, held in Manta, Ecuador. IUCAF will contribute on the protection of radio astronomy observations at around 79 GHz.

IUCAF member, A. Tzioumis, is the Chair of ITU-R Working Party 7D (radio astronomy). And IUCAF member, H. Chung, is the vice-chairman of ITU-R Study Group 7 (Science Services).

6. Contact with the Sponsoring Unions and ICSU

IUCAF maintains regular contact with its supporting Scientific Unions and with ICSU. The Unions play a strong supporting role for IUCAF and the membership is greatly encouraged by their support. IUCAF continued its activities towards strengthening its links with other passive radio science communities, in particular in space science, and defining a concerted strategy in common spectrum management issues.

IUCAF held a business meeting during the IAU General Assembly in Beijing, China. The details can be found in section 4.

The IUCAF chair, M. Ohishi, was the president of IAU Commission 5 on Documentation and Astronomical Data until August 2012. IUCAF member, W. van Driel, was the president of IAU Commission 50 until August 2012. Two IUCAF members, A. Tzioumis and M. Ohishi, are appointed the Organising Committee (OC) members of IAU Commission 50. M Ohishi is also an OC member of IAU Commission 51 (Bioastronomy). M. Ohishi chairs the Working Group on Astrophysically Important Spectral Lines under Division B, IAU. He is also appointed the official liaison between the IAU and the ITU, and a member of WG Redefinition of UTC, Division A, IAU. IUCAF member, S. Ananthakrishnan, is the president of URSI Commission J (radio astronomy).

7. Publications and Reports

IUCAF has a permanent web address, http://www.iucaf.org, where the latest updates on the organization's activities are made available. All contributions to IUCAF-sponsored meetings are made available on this website.

8. Conclusion

IUCAF interests and activities range from preserving what has been achieved through regulatory measures or mitigation techniques, to looking far into the future of high frequency use, giant radio telescope use and large-scale distributed radio telescopes. Current priorities for the coming years are: the protection of radio astronomy observations from collision avoidance radars at around 79 GHz region, high-frequency power line communications (HF-PLC) on all passive services, and studies on the operational conditions that will allow the successful operation of future giant radio telescopes.

IUCAF plans to hold the 4th Summer School on Spectrum Management in 2013 or 2014; its possible venue is Santiago, Chile. IUCAF has saved its budget for supporting young scientists and engineers at the planned summer school, who are expected to work together in future. If this summer school is actually held in Chile, it would be a very good opportunity for radio scientists in the South America to learn how to protect radio quiet environment that is needed for the passive radio science services.

IUCAF is grateful for the moral and financial support that has been given for these continuing efforts by ICSU, URSI, IAU and IAU during the recent years. IUCAF also recognizes the support given by radio astronomy observatories, universities and national funding agencies to individual members in order to participate in the work of IUCAF.

Masatoshi Ohishi, IUCAF Chair
IUCAF website : http://www.iucaf.org
IUCAF contact : iucafchair@iucaf.org

Eigenanalysis of Open Radiating, Periodic, and Curved Waveguide Structures

G.A. Kyriacou, C.S. Lavranos
P.C. Allilomes, C. Zekios
S. Lavdas, A.V. Kudrin

Abstract

A review of our research efforts on the eigenanalysis of open radiating and closed structures, straight as well as curved, is presented herein. The elaborated geometries were arbitrarily shaped and loaded in general with inhomogeneous and/or anisotropic media. The initial effort was focused on two-dimensional (2-D) waveguide structures. A particular focus was on open radiating waveguides including leaky-wave phenomena, as well as geometries curved in the transverse direction, and possibly curved along the direction of propagation. The current efforts are twofold. The first is to extend the methodologies for the eigenanalysis of three-dimensional structures (open or closed cavities and antennas), including external and particularly characteristic modes and the related radiation phenomena. The second aim refers to the establishment of an eigenanalysis tool for periodic structures loaded with anisotropic or artificial media, addressing bandgap and frozen modes.

1. Introduction

The modal characteristics of waveguide structures are essential for the design of a variety of microwave devices. Valuable analytical solutions of closed waveguides with canonical cross sections have been well established since the early days of microwaves. Arbitrary cross-section waveguides, partially or inhomogeneously loaded with either isotropic or anisotropic materials, can also be studied with the aid of numerical techniques such as the Finite-Element Method (FEM) or Finite-Difference methods (FD), e.g. [1, 2].

From the first step of this effort, a hybrid Finite Element Method in conjunction with a cylindrical-harmonic expansion was established for the analysis of open waveguides. The transparency of the fictitious circular contour truncating the finite-element mesh was ensured by enforcing the field continuity conditions according to a vector Dirichlet-to-Neumann mapping (DtN) [1]. The eigenanalysis of curved waveguides was confronted by a finite-difference frequency-domain (FDFD) method, formulated in orthogonal curvilinear coordinates [2]. The latter eliminated the usually encountered staircase effects by making the grid conformal to the material's boundaries. Additionally, the method's frequency-domain formulation supported multi-coordinate systems and inhomogeneous grids, enabling fine mesh around current-carrying conductors, and coarse mesh in the area of low field variations. These features offer high accuracy with minimum computer resources.

Aiming at the eigenanalysis of electrically large three-dimensional structures, such as reverberation chambers or focused microwave cavities, the initial finite-element eigenanalysis formulation was accordingly extended [3]. For this purpose, the perturbations (small objects) inside the cavity were enclosed within a canonically shaped fictitious surface, and the interior field was described using a vector FEM. Outside these perturbations, within the large canonical cavity, the electromagnetic field was represented as an expansion of the analytical eigenfunctions. The field continuity across the fictitious surface was exactly enforced according to the Dirichlet-to-Neumann formalism to yield an appropriate eigenvalue problem. This is was in turn solved for the resonant frequencies and the related quality factors. Within this effort, we are currently working towards extending this methodology for the eigenanalysis of open cavities, including various types of cavity-backed antennas. Particular attention is devoted to the formulation of external and characteristic-mode eigenproblems, which offer clear physical insight, enabling researchers to devise novel

G. A. Kyriacou, P. C. Allilomes, C. Zekios, and S. Lavdas are with the Democritus University of Thrace, Department of Electrical & Computer Engineering, Microwaves Lab, Xanthi, Greece; e-mail: gkyriac@ee.duth.gr. C. S. Lavranos is with the Department of Electrical Engineering, Kavala Institute of Technology, Kavala, Greece. A. V. Kudrin is with the University of Nizhny Novgorod, Department of Radiophysics, Nizhny Novgorod, Russia.

This is an invited paper from Commission A.

structures. Numerous challenging problems are encountered in efficiently handling these types of problems. In particular, when conductor losses are included through an impedance boundary condition, the eigenproblem becomes nonlinear. A methodology of evaluating the effects of losses and, particularly, the quality factors within practical accuracies by just solving the linear eigenproblem resulting from perfect electric boundary conditions was devised by our group [4]. Besides that, a novel approach using the orthogonality of eigenfunctions was worked out, based on field equivalence principles; it will also separately presented.

The design of a variety of periodic structures, such as filters, frequency-selective surfaces, and traveling-wave antennas, can be served very efficiently though the knowledge of the associated propagation constants and characteristic impedances of the modes. Motivated by these requirements, our previous FEM and frequency-domain finite-difference eigenanalysis methods have now been appropriately extended to account for the periodicity [5]. Infinite periodicity was first assumed, reducing the electromagnetic analysis to that of a single period or a unit cell. Initially, the classical approach of periodic boundary conditions (PBC) was adopted by enforcing them on the periodic surfaces of the unit cell. Performing a series of numerical experiments, it was soon realized that the periodic-boundary-condition approach had some serious limitations, since the resulting eigenvalues (propagation constants) presented large deviations from their true values when the phase differences between the periodic surfaces exceeded a limit between 140° to 180°. This error was more pronounced when full tensor anisotropic materials, such as magnetized ferrites or anisotropic dielectrics, were involved (e.g., as in frozen-mode structures). Learning from some analytical eigenanalysis methodologies usually worked out in the optical regime, we decided to incorporate the Floquet expansion within the frequency-domain finite-difference formulation. The resulting approach indeed performed very well, enabling even the prediction of "frozen modes" with high accuracy.

However, even this approach was limited to an ω or k_0 formulation where the dispersion curves were evaluated by scanning the propagation constant (β) range of values. However, this was possible when β was real, and only for certain simple geometries. For arbitrary geometries and anisotropic material loadings, and especially for lossy and open radiating structures, the eigenvalue, β, was complex, and its range was unknown. For this purpose, we put effort into formulating a β eigen-problem. However, a new serious challenge occurred, since the resulting eigen-problem was highly nonlinear, and hence it could not be directly solved. Trying to work this out, the corresponding linear eigen-problem was first formulated and solved, where both radiation and Joule-heating losses were ignored to restrict β to real values. In turn, this linear eigen-problem was formulated and solved following an ω formulation to yield the whole spectrum of approximate eigenvalues. These were then used as starting values for the actual nonlinear β eigen-problem, and trimmed using an iterative approach. Besides that, in certain particular cases when approaches like the transfer matrix were adopted, they ended up in a linear formulation. Hence, an effort was started to reformulate the problem in a step-by-step procedure aimed at an inherently linear formulation. Moreover, the next step in the eigenanalysis efforts aimed at formulations for external or characteristic modes, but based on FEM or frequency-domain finite-difference methods (instead of MoM), in order to account for anisotropic inhomogeneous material loadings. In parallel to the eigenanalysis efforts, work towards exploiting the numerical eigenfunctions as "entire-domain basis functions" within full-wave simulators was started. The ambitions were directed toward the efficient study of electrically large and finite periodic structures.

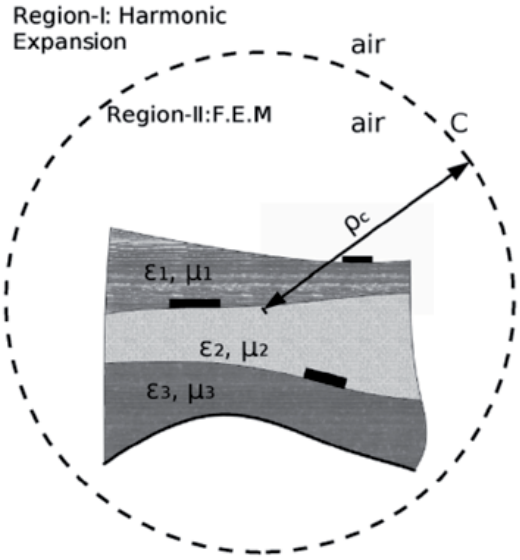

Figure 1. A general open radiating waveguide geometry.

2. Methodology for Waveguide Structures

The two eigenanalysis methodologies (FEM and the Frequency-Domain Finite-Difference Method) for addressing arbitrary waveguide structures will be reviewed next. For each method, the rationale is given, aiming at emphasizing the method's strengths and weakness, along with its applicability.

2.1 Hybrid Finite-Element Method for Open Waveguides

The geometry of an arbitrary cross section, inhomogeneously loaded open waveguide structure, enclosed within a circular separation contour, C, is shown in Figure 1. Time-harmonic fields using $e^{j\omega t}$ and propagation along the *z* axis using $e^{-j\beta z}$ are assumed. The field vectors as well as the nabla operator are separated into transverse

(subscript t) and longitudinal components (z components) as

$$\vec{\mathrm{E}} = \vec{\mathrm{E}}_t + E_z \hat{z}\,, \tag{1}$$

$$\vec{\nabla} = \vec{\nabla}_t + \frac{\partial}{\partial z}\hat{z}\,. \tag{2}$$

Inside the contour C (Region II), the vector wave equation for the electric field is considered, and the standard Galerkin procedure is applied to yield a weak formulation of the form [1]

Bounded Region II:

$$\iint_{S_{II}} \frac{1}{\mu_r}\left[\left(\vec{\nabla}_t \times \vec{T}_t\right)\bullet\left(\vec{\nabla}_t \times \beta\vec{E}_t\right) + \beta^2 \vec{T}_t \bullet \vec{\nabla}_t\left(-jE_z\right)\right] ds$$

$$+\iint_{S_{II}} \frac{1}{\mu_r}\beta^2 \vec{T}_t \bullet \left(\beta\vec{E}_t\right) ds \tag{3}$$

$$= k_0^2 \iint_{S_{II}} \varepsilon_r \vec{T}_t \bullet \left(\beta\vec{E}_t\right) ds - \underbrace{\oint_C \frac{1}{\mu_r}\vec{T}_t \bullet \left(\hat{n}\times\vec{\nabla}_t \times \beta\vec{E}_t\right) dl}_{I_A}$$

$$\iint_{S_{II}} \frac{1}{\mu_r}\left[\vec{\nabla}_t T_z \bullet \vec{\nabla}_t\left(-jE_z\right) + \vec{\nabla}_t T_z \bullet \beta\vec{E}_t\right] ds$$

$$= k_0^2 \iint_{S_{II}} \varepsilon_r T_z\left(-jE_z\right) ds \tag{4}$$

$$+\underbrace{\oint_C \left[\frac{1}{\mu_r} T_z \frac{\partial\left(-jE_z\right)}{\partial n} + T_z \hat{n} \bullet \left(\beta\vec{E}_t\right)\right] dl}_{I_B},$$

where $\vec{T} = \vec{T}_t + T_z\hat{z}$ is the vector weighting function, and S_{II} is the area of the bounded region, II. The contour integrals, I_A and I_B, along the fictitious contour C constitute the means for coupling the FEM field inside C to the field expansion outside C. This coupling strictly follows the vector Dirichlet-to-Neumann (DtN) mapping.

The field in the unbounded region, I, is expressed as a superposition of TE_z and TM_z modes, which, according to the classical textbook of Jackson [6], constitute a complete set of vector solutions to Maxwell's equations. The longitudinal components in unbounded Region I read

$$\mathrm{TM}_z\colon\ E_z^e(\rho)\Big|_{\rho\geq\rho_c} = \sum_{m=-\infty}^{+\infty} A_m e^{-jm\varphi} H_{|m|}^{(2)}\left(k_\rho\rho\right) \tag{5}$$

$$\mathrm{TE}_z\colon\ H_z^e(\rho)\Big|_{\rho\geq\rho_c} = \sum_{m=-\infty}^{+\infty} B_m e^{-jm\varphi} H_{|m|}^{(2)}\left(k_\rho\rho\right) \tag{6}$$

where $k_\rho = \sqrt{k_0^2 - \beta^2}$ is the radial wavenumber, and $H_{|m|}^{(2)}$ is the Hankel function of the second kind.

Following a standard waveguide analysis, e.g., Pozar [7], the transverse field components are expressed in terms of their axial counterparts in Equations (5) and (6) by expanding Maxwell's curl equations in Cartesian coordinates [1].

For the coupling of the field expression inside and outside C, the vector Dirichlet-to-Neumann principles are in turn applied. The first step requires that "the solution in the unbounded region, I, be constructed from Dirichlet data on the separation contour, C." Since the electric-field wave equation is solved using the FEM in the interior of C, then the Dirichlet data are comprised of the tangential field components, $E_z^{(FEM)}$ and $E_\varphi^{(FEM)}$. The related field continuity conditions hence read

$$E_z{}^{\mathrm{e}}(\rho)\Big|_{\rho=\rho_c} = E_z^{(FEM)}\Big|_{\rho=\rho_c}\,, \tag{7}$$

$$E_\varphi{}^{e}(\rho)\Big|_{\rho=\rho_c} = E_\varphi^{(FEM)}\Big|_{\rho=\rho_c}\,. \tag{8}$$

Exploiting the orthogonality properties of the azimuthal eigenfunctions $e^{-jm\varphi}$, the unknown coefficients, A_m and B_m of the expansion are evaluated [1] through Equations (7) and (8). This step has indeed established the solution in the unbounded domain (Region I). The Dirichlet-to-Neumann second step reads "establish a Dirichlet-to-Neumann map on the separation contour, C, by differentiating the solution in the unbounded domain with respect to the transverse radial ρ coordinate, and enforce their continuity across C." Since the Dirichlet data are comprised of the electric field, the differentiation with respect to the ρ coordinate is given by the Maxwell curl equation, $\vec{\nabla}\times\vec{E}^e$, which yields the tangential magnetic-field components all over Region I: H_z^e and H_φ^e. The H_z^e, H_φ^e values on the C contour comprise the Neumann data. Their availability enables the evaluation of the coupling integrals, I_A and I_B, through the enforcement of the tangential magnetic-field continuity:

$$H_z^{(FEM)}\Big|_{\rho=\rho_c} = H_z^{(e)}\Big|_{\rho=\rho_c}, \quad (9)$$

$$H_\varphi^{(FEM)}\Big|_{\rho=\rho_c} = H_\varphi^{(e)}\Big|_{\rho=\rho_c}. \quad (10)$$

The coupling integrals, I_A and I_B, of the weak formulation of Equations (3) and (4) are then rewritten by means of Maxwell's curl equations in cylindrical coordinates as

$$I_A = \mathrm{j}\omega\mu_0 \oint_C \vec{T}_t \bullet \left(\beta H_z \hat{\varphi}\right) dl, \quad (11)$$

$$I_B = \omega\mu_0 \oint_C T_z H_\varphi dl. \quad (12)$$

The substitution of Equations (9) and (10) into Equations (11) and (12), and through that in Equations (3) and (4), concludes with the final "equivalent closed hybrid FEM formulation." This is in turn discretized over the whole Region II, including the contour C, using the interpolation functions for hybrid edge/node triangular elements (line elements for C), according to [8]. The resulting expressions are then separated into a group of terms involving the unknown eigenvalue (β) and terms independent of that, to yield a nonlinear generalized eigenvalue problem [1]:

$$A(k_0, \beta) \bullet [e] = 0. \quad (13)$$

The eigenvalues of Equation (13) are the complex propagation constants of the waveguide structure.

2.1.1 Discussion of Uniqueness

It is worth noting that the Dirichlet-to-Neumann procedure described above contradicts the electromagnetic uniqueness theorem, which states that the enforcement of the continuity of either the tangential electric field or the tangential magnetic field on the contour C yields a unique solution. To the contrary, Dirichlet-to-Neumann presumes the enforcement of both electric and magnetic field continuity. However, the Dirichlet-to-Neumann provisions were indirectly well established by Prof. Harrington in 1989 [9], who stated that enforcement of both conditions is absolutely necessary in order to avoid matrix singularities at the frequencies of internal resonances. At this point, one may recall that the propagation constants are the solutions of some kind of a characteristic equation, which is identical to the transverse resonance condition. This hence is indeed a condition of internal resonance, and both tangential electric and magnetic field continuity conditions must be enforced.

2.1.2 Nonlinearity and Equivalent Linear Eigen-Problem

Equation (13) represents a nonlinear generalized eigen-problem, since the unknown eigenvalue (β) occurs in multiple terms, but also within the argument $k_\rho = \sqrt{k_0^2 - \beta^2}$ of the Hankel functions in Equations (5) and (6). For the solution of Equation (13) a good initial guess is inevitable, which can in turn be improved by employing a *matrix regula falsi* method [10]. The necessary starting solutions are obtained by solving an approximate linear eigenvalue problem. The latter is established by approximating the argument of the Hankel functions involved in the field expansion in the unbounded Region I as

$$k_\rho \rho = \rho\sqrt{k_0^2 - \beta^2}\Big|_{(\beta/k_0)^2 << 1} \approx k_0 \rho. \quad (14)$$

This approximation yields a linear eigenvalue problem that is solved by employing the Arnoldi algorithm [11], which efficiently handles the sparse matrices involved. Although this approximation was expected to work well around $\beta/k_0 \to 0$, it has however proven to perform quite well for β/k_0 up to 0.8 [1]. This makes it a valuable tool for the study of leaky waveguide structures, since a single solution of the linear eigenvalue problem yields the entire spectrum of the complex propagation constants. It will also be shown in the numerical-results section that the results of the linear approximation only require improvement using the nonlinear eigenvalue formulation around the frequency ranges of high leakage (attenuation) constants. The method was validated against published numerical and experimental results, and new open waveguide structures have been studied.

2.1.3 Future Improvements

The major limitation of the above method is related to the high computational cost of the "global radiation condition" resulting from the enforcement of the artificial truncation contour's (C) transparency through the Dirichlet-to-Neumann approach. One part of this is unavoidable, which is related to the creation of a dense area within the otherwise sparse system matrix, and this is inherent to global transparency conditions. This is actually the cost to be paid for the gain of an accurate transparency condition. However, most of the additional computations are devoted to the calculation of the integrals along the artificial contour C.

2.2 FDFD Method in Orthogonal Curvilinear Coordinates

Even though the above FEM methodology performs very well, major difficulties occur when a full tensor anisotropic media loading is involved. An alternative,

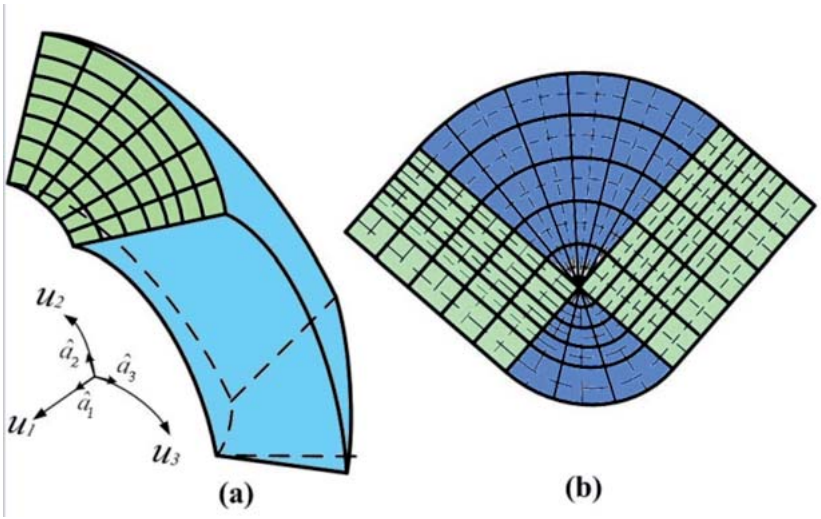

Figure 2. (a) The discretization of an arbitrary waveguide structure in orthogonal curvilinear coordinates; (b) A combination of different coordinate systems (multi-grid).

more-convenient method was thus sought. In view of the above, this research effort was based on a two-dimensional finite-difference frequency-domain (2D-FDFD) eigenvalue method, formulated in orthogonal curvilinear coordinates. The detailed theoretical basics and a variety of applications have been presented in our previous work, e.g., [2, 12-14]. The two-dimensional frequency-domain finite-difference scheme aims at the formulation of an eigenvalue problem for the propagation constant of waveguide structures in orthogonal curvilinear coordinates (u_1, u_2, u_3), as shown in Figure 2. The cross section of the waveguide structure can be of arbitrary geometry, loaded with inhomogeneous and, in general, anisotropic materials, described by dielectric permittivity and magnetic permeability tensors generally defined as

$$\bar{\bar{\varepsilon}} = \begin{bmatrix} \varepsilon_{11} & \varepsilon_{12} & \varepsilon_{13} \\ \varepsilon_{21} & \varepsilon_{22} & \varepsilon_{23} \\ \varepsilon_{31} & \varepsilon_{32} & \varepsilon_{33} \end{bmatrix}, \qquad (15)$$

$$\bar{\bar{\mu}} = \begin{bmatrix} \mu_{11} & \mu_{12} & \mu_{13} \\ \mu_{21} & \mu_{22} & \mu_{23} \\ \mu_{31} & \mu_{32} & \mu_{33} \end{bmatrix}.$$

The analysis starts from Maxwell's curl equations for the electric and magnetic intensity fields in the frequency domain, considering a time-harmonic dependence as $e^{+j\omega t}$, while sources are omitted since an eigenvalue-problem formulation is sought. The method is formulated as a two-dimensional problem, and thus a uniform cross section is assumed. Moreover, the curvature along the propagation direction must be constant in order to justify wave propagation with an invariant phase constant [15], namely, in order to ensure a linear phase variation in the u_3 direction. All metric coefficients must thus be independent of u_3 [15]. The coordinate systems that comply with these restrictions are the Cartesian, the cylindrical (parabolic, bipolar, or elliptic cylindrical), the elliptic, and the parabolic coordinate systems [2]. This limitation restricts the analysis to specific geometries depending on the coordinate systems describing them, but it is rather an inherent physical than a numerical-modeling limitation. It is important to notice that a frequency-domain method is capable of combining different coordinate systems with a proper multi-grid formulation in order to describe more-complex geometries, as shown in Figure 2b.

2.2.1 Operator Discretization

After some algebraic operations, one may conclude with the compact form of the curl operator:

$$\bar{\nabla} \times \bar{E} = -j\omega \bar{\bar{\mu}} \bar{H} = -j\omega \bar{B} \quad \rightarrow$$

$$\begin{Bmatrix} -(j\beta)\left(\frac{1}{h_3}\right)\hat{\alpha}_3 \times (\bullet) & -\hat{\alpha}_3 \times \left[\left(\frac{1}{h_3}\right)\bar{\nabla}_{tc}(\bullet)\right] \\ -\bar{\nabla}_{tc} \bullet \hat{\alpha}_3 \times (\bullet) & 0 \end{Bmatrix} \begin{pmatrix} \bar{E}_t \\ h_3 E_3 \end{pmatrix} \qquad (16)$$

$$= -j\omega \begin{pmatrix} \bar{\bar{\mu}}_{tt} & \bar{\mu}_{tl} \\ \bar{\mu}_{lt} & \mu_{ll} \end{pmatrix} \begin{pmatrix} \bar{H}_t \\ H_3 \end{pmatrix}$$

$$= -j\omega \begin{pmatrix} \bar{B}_t \\ B_3 \end{pmatrix}.$$

Likewise, its dyadic expression representing the curl of magnetic field is obtained. These two expressions are in turn discretized with the aid of a curvilinear grid over the whole solution domain, according to the basic principles of Yee's grid, and employing a central finite-difference

scheme. In this manner, a curvilinear discretization will be applied to the whole solution domain.

These discretized forms are then formulated as a nondeterministic eigen-problem of the form $[A][u] = \beta[u]$ Vector $[u]$ is the eigenvector, and β is the sought eigenvalue. Matrix $[A]$ consists of submatrices that represent the discrete form of the basic operators, such as the gradient and the divergence. Every operator is discretized with respect to the curvilinear mesh, formulated in a matrix form representing the whole solution domain, and modifies the system via a simple matrix multiplication. In turn, the two curl equations are written as systems of equations like Equation (16):

$$\begin{bmatrix} -(j\beta)\left(\frac{1}{h_3}\right)\boldsymbol{A_{te}} & -\boldsymbol{A_{te}}\left(\frac{1}{h_3}\right)\bullet\boldsymbol{G_{cet}} \\ -\boldsymbol{D_{cmt}}\bullet\boldsymbol{A_{te}} & 0 \end{bmatrix} \begin{bmatrix} \mathring{\mathrm{A}}_{\mathrm{t}} \\ \mathrm{h}_3\mathbf{E_3} \end{bmatrix}$$

$$= -j\omega \begin{pmatrix} \boldsymbol{M_{tt}} & \boldsymbol{M_{tl}} \\ \boldsymbol{M_{lt}} & \boldsymbol{M_{ll}} \end{pmatrix} \begin{pmatrix} \boldsymbol{\zeta_t} \\ \boldsymbol{H_3} \end{pmatrix}. \qquad (17)$$

All the quantities involved are either matrices or vectors. Subscripts *e* and *m* denote operators-matrices acting on electric and magnetic field components, respectively. These are different, since they are discretized on different grids (shifted by a half cell). Subscripts *c*, *t*, and *l* refers to curvilinear, transverse, and longitudinal, respectively. For instance, $\boldsymbol{G_{cet}}$ and $\boldsymbol{D_{cet}}$ are the transverse curvilinear gradient and divergence operators corresponding to the electric field, while $\boldsymbol{A_e}$ represents the cross operator $\hat{\alpha}_3 \times (\bullet)$, and $\boldsymbol{M_{xy}}$ represents the permeability tensor $\overline{\overline{\mu}}_r$. The boundary conditions are incorporated into this system by proper modification of the submatrices involved. Considering metallic boundaries as perfect electric conductors, all corresponding tangential electric-field components are thus set equal to zero through the elimination of specific lines from the basic submatrices. Due to the sparsity of matrices involved, the final eigenvalue problem is solved using the Arnoldi Algorithm [16].

As mentioned above, this method can be formulated with nonuniform grids, which is essential for the description of curvilinear structures with fine geometry features as clearly shown in [12]. Critical fine details, such as metallic strip conductors, ask for a dense-enough grid in order to ensure their accurate description. However, such a grid may dramatically increase the dimensions (rank) of the system matrix, which requires excessive computational resources as well as increased simulation time. The nonuniform adaptive discretization is a smart technique that solves that problem. The whole grid can be comprised of fine and coarse curvilinear areas, depending on the position of the fine features. The number of segments may thus be the same as in a coarse grid, but their step sizes vary following the geometry of the problem. This modification makes sense, keeping in mind that the finite-difference frequency-domain methods are stable even when the step size is not the same everywhere in the grid. Additionally, for the simulation of geometries with arbitrary cross section, the two-dimensional curvilinear frequency-domain finite-difference multi-grid formulation was developed [13]. In particular, the method is modified to accurately combine more than one orthogonal curvilinear grid for the description of complex arbitrary geometries. This is necessary in order to retain a grid conformal to the boundaries all over the guiding structure's cross section. Finally, the complex matrix format ability enables the introduction of the well known PML complex tensor [14].

The latter gives the ability of simulating open radiating geometries, as was shown in [14]. However, it suffers from spurious solutions created by the imperfect transparency of the PMC contour, also known as Berenger modes [14]. Summarizing, the frequency-domain finite-difference method has been used to accurately extract the propagation constants of several curved structures, such as curved rectangular, cylindrical, or coaxial waveguides or microstrip geometries.

2.2.2 Limitations and Future Extension of the FDFD Eigenanalysis

There are two major limitations of the present implementation of this frequency-domain finite-difference eigenanalysis. The first is inherent to its dual electric and magnetic field grids, resulting from the Yee-type cell. As shown explicitly in Figure 2, the two grids are shifted by a half cell. When modeling a nonmagnetic inhomogeneous dielectric, its boundaries should hence coincide with the E-field grid lines. Likewise, for the discretization of a non-dielectric magnetic media, its boundaries must coincide with the H-field grid lines. However, most practical anisotropic media (such as ferrites or multiferroics) present inhomogeneous entries in both their $\overline{\overline{\varepsilon}}_r$ and $\overline{\overline{\mu}}_r$ tensors: there hence will be a half-cell inaccuracy in their modeling. Being aware of the deleterious effects of discretization inaccuracies on the eigenvalues and eigenvectors, we worked toward removing this limitation. Among the candidate solutions examined was the so-called "condensed node" approach. The other serious limitation refers to the adoption of an "exact" global unbounded domain truncation method, in order to eliminate the fictitious "Berenger modes" occurring when techniques like PML are utilized. A global radiation condition exploiting the vector Dirichlet-to-Neumann approach as described in the FEM methodology is under investigation.

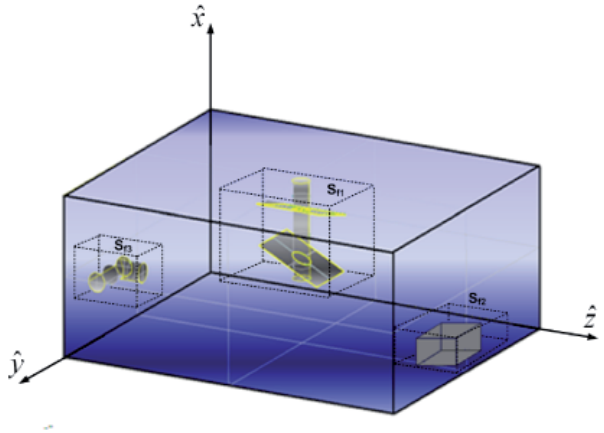

Figure 3. A reverberation chamber, including a mode stirrer, an antenna, and the equipment under test (EUT).

2.3 A Hybrid Domain FEM and Eigenfunction Expansion Method for Electrically Large Cavities

This hybrid technique is directed toward the application of the Finite-Element Method, similar to the by-moment method but extending it so that an eigenvalue formulation is attained. Each *i*th perturbation is enclosed inside a fictitious parallelepiped surface S_f (fictitious box) (see Figure 3), and the electromagnetic field is expressed by employing the Finite-Element Method. Aiming at a general formulation, the electromagnetic behavior within the perturbed region (Domain II) is characterized by the electric-field vector wave equation, which for a source-free region with tensor permittivity ($\bar{\bar{\varepsilon}}_r$) and permeability ($\bar{\bar{\mu}}_r$) materials reads

$$\nabla \times \bar{\bar{\mu}}_r^{-1} \bullet \nabla \times \bar{E} - k_0^2 \bar{\bar{\varepsilon}}_r \bar{E} = 0 . \qquad (18)$$

Applying the standard Galerkin procedure to Equation (18), the following weak formulation can be derived [17]:

$$\iiint \left(\nabla \times \bar{T}\right) \bullet \bar{\bar{\mu}}_r^{-1} \bullet \nabla \times \bar{E} dV - k_0^2 \iiint \bar{T} \bullet \bar{\bar{\varepsilon}}_r \bar{E}$$

$$- jk_0 \oiint_S \bar{T} \bullet \left(\hat{n} \times \bar{H}\right) dS = 0 , \qquad (19)$$

where $k_0 = \omega/c$ is the free-space wavenumber, *T* is the vector weighting function, and *V* denotes the space of the perturbed region enclosed inside the S_f (Figure 3). The surface integral appearing in the weak form provides the means to combine the FEM solution with the field expansion in the unperturbed region. In the unperturbed cavity domain (I), outside the surface S_f, the field is expanded into an "infinite" sum of the analytically available eigenfunctions/ eigenmodes of an empty rectangular cavity, obtained considering perfect electrically conducting (PEC) walls. These modes constitute a complete set of vector solutions of Maxwell's equation, provided that there is not any mode degeneration (e.g., Jackson [5], and specifically [18]):

$$E_z^I(x,y,z) = \sum_Q \left\{ B_{pqr}^e \sin\left(\frac{p\pi}{u}x\right) \sin\left(\frac{q\pi}{v}y\right) \cos\left(\frac{r\pi}{w}z\right) \right\} \qquad (20)$$

$$H_z^I(x,y,z) = \sum_Q \left\{ B_{pqr}^h \cos\left(\frac{p\pi}{u}x\right) \cos\left(\frac{q\pi}{v}y\right) \sin\left(\frac{r\pi}{w}z\right) \right\} \qquad (21)$$

where the mode indexes are defined by (p,q,r). The transverse components can be easily expressed in terms of the above *z* components using the classical analysis of rectangular cavities.

At this point, the most serious difficulty occurring within this type of hybrid methodologies is the necessity to decouple the degrees of freedom in the numerical and analytical expansions. For this purpose, a type of "by-moment" approach (an intermediate continuity condition) is employed by considering equivalent electric and magnetic current densities on these fictitious surfaces, which result from Love's Equivalence Principle. These equivalent currents are expanded into either "local" (on each surface) or "global" all over the box (the small empty box eigenfunctions) orthogonal eigenfunctions. According to Dirichlet-to-Neumann, the electric-field continuity is first enforced in two steps: through the equivalent magnetic current to establish the cavity (Domain I) solution in terms of that of the box Domain II:

$$\vec{M}^{\exp} = \vec{M}^{FEM} \Leftrightarrow \hat{n} \times \bar{E}^{\exp} = \hat{n} \times \bar{E}^{FEM} . \qquad (22)$$

Namely, the unknown coefficients B^e and B^h involved in Equations (20) and (21) must be isolated, and in turn evaluated. This is carried out using appropriate testing functions, exploiting the orthogonality properties of an equivalent current expansion in trigonometric eigenfunctions. For that reason, an intermediate step is required, where an orthogonal base is constructed exploiting the nature of the fictitious surface. The course to define an orthogonal basis function over S_f is equivalent to a two-dimensional Fourier transform. From a different point of view, it was realized that it was possible to adopt the field expansion (TE and TM) modes of a cavity with PEC walls for the representation of J_{eq}. Correspondingly, the field expansion (TE and TM) of a cavity (identical to the box, S_f) with perfect magnetic walls (PMC) is utilized for $\vec{M}_{eq}$ Next, the Dirichlet-to-Neumann technique is applied to bind the solutions of the corresponding subdomains, moving from the inner to the outer region. For this purpose, only the electric field or $\vec{M}_{eq}$ continuity is enforced, and thus

only the equivalent expansion of the perfect magnetic conductor (PMC) cavity is required:

$$E_z^{II^{\exp}}(x,y,z)=\sum_P\left\{A_{nml}^e\cos\left(\frac{m\pi}{a}x\right)\cos\left(\frac{n\pi}{b}y\right)\sin\left(\frac{l\pi}{d}z\right)\right\} \tag{23}$$

$$H_z^{II^{\exp}}(x,y,z)=\sum_P\left\{A_{nml}^h\sin\left(\frac{m\pi}{a}x\right)\sin\left(\frac{n\pi}{b}y\right)\cos\left(\frac{l\pi}{d}z\right)\right\} \tag{24}$$

where P is a cumulative mode index defined by (m,n,l). The above procedure is actually a type of "by-moment" approach used to decouple the required number of modes for the field expansion in the large cavity from the FEM mesh degrees of freedom over the small box cavity surface, S_{fi}. The equivalent currents over the small box surface can be assumed to act as generating the fields in the large cavity Region I. According to the Dirichlet-to-Neumann formalism, the modal amplitudes of cavity modes in Region I must be determined by enforcing the continuity of the electric field across the surface (Dirichlet data along S_{fi}), initially between FEM and the interior expansion:

$$\hat{n}\times\overline{E}^{II\exp}=\hat{n}\times\overline{E}^{FEM}, \tag{25}$$

and in turn (by-moment) between the surface S_{fi} (II) and the exterior cavity volume (I) expansion:

$$\hat{n}\times\overline{E}^{II^{\exp}}=\hat{n}\times\overline{E}^{I^{\exp}}. \tag{26}$$

Regarding the unknown coefficients A^e and A^h given in Equations (23) and (24), these are first isolated and then evaluated by exploiting the orthogonality property of the trigonometric functions in Equations (25). The coefficients thus read[1]

$$A^e=\iint_S(\ldots)E^{FEM}dS \tag{27}$$

$$A^h=\iint_S(\ldots)E^{FEM}dS.$$

Now, imposing one more time the orthogonality property of the trigonometric functions on Equation (27), the coefficients A^e and A^h are expressed in a formal was as[1]

$$A^e=\iint_S(\ldots)E^{I^{exp}}dS \tag{28}$$

$$A^h=\iint_S(\ldots)E^{I^{exp}}dS.$$

Equations (25) and (26), resulting in Equations (27) and (28), represent the realization of the by-moment approach, where some N degrees of freedom in the FEM over the box surface S_f are transferred to Q modal expansions and, in turn, are transferred to P modes of the large cavity.

As it occurs from Equations (27) and (28), the field of the exterior domain is absolutely related to the field described by the FEM through the analytical expansion of Domain II. From Equations (27) and (28), the unknown coefficients B^e and B^h are thus totally defined. Now, according to the second step of the Dirichlet-to-Neumann formalism, the field in the unperturbed Domain I is differentiated in order to establish the Dirichlet-to-Neumann map, so as to obtain the Neumann data along the separation surface. This differentiation is actually provided by the electric-field curl equation, itself. The curl of the electric field is thus considered to yield the magnetic-field expressions in the unperturbed domain, as well as along the separation surface, S_f:

$$H^I=\iint_S(\ldots)E^{FEM}dS. \tag{29}$$

The third Dirichlet-to-Neumann step asks for the enforcement of the continuity of the derivatives along S_f This herein reads as requiring the tangential components of the magnetic-field expansion to be equal to those of the FEM description along the separation surface:

$$\hat{n}\times\overline{H}^{exp}=\hat{n}\times\overline{H}^{FEM}. \tag{30}$$

These tangential magnetic-field components are identical to the field derivatives occurring in the surface integrals of the FEM mesh formulation of Equation (19). The surface integral of the FEM can thus be derived by exploiting the Dirichlet-to-Neumann map:

$$S=jk_0Z_0\sum_Q\left[\Phi(k_0,1/k_0)\iint\overline{T}\bullet\hat{n}dS\right], \tag{31}$$

where $\Phi(k_0,1/k_0)$ is a factor involving either terms of k_0 or $1/k_0$. The resulting system of equations is in turn formulated into a generalized eigenvalue problem by separating the terms involving the free-space wavenumber, k_0. The final matrix form can be written as

$$[S_{el}][e]-k_0^2[T_{el}][e]-jk_0^2[S_{f1}][e]-j[S_{f2}][e]=[0] \tag{32}$$

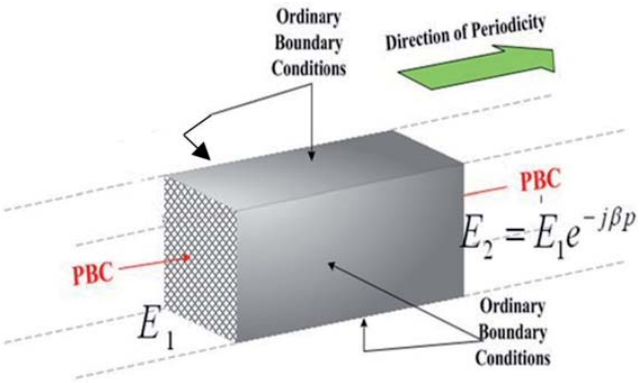

Figure 4. The analysis of an infinite periodic structure is replaced by that of a unit cell.

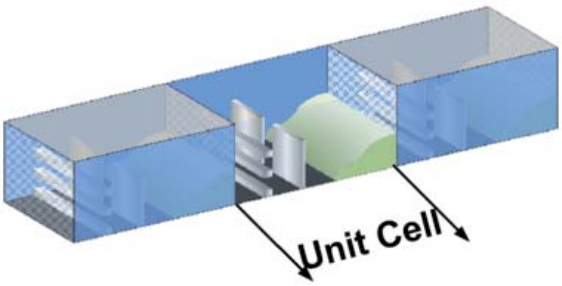

Figure 5. A three-dimensional unit cell with arbitrary inhomogeneities in all three directions.

It is important to note that the above generalized eigenvalue problem retains just a few hundreds of degrees of freedom, instead of the millions required by a brute-force discretization. This is actually formulated and solved for the cavity resonant frequencies and the corresponding eigenfunctions.

2.3.1 Limitations and Future Extensions

As in the FEM for open waveguides presented in the first section, the major limitation of this method is related to the high computational resources required to enforce the Dirichlet-to-Neumann field continuity over the fictitious boxes enclosing the inhomogeneties. A novel approach, based on the orthogonality properties of the whole-cavity eigenfunctions in conjunction with a field equivalence approach, is under consideration (soon to be submitted for publication), which is expected to efficiently address this limitation. The main extension of the presented methodology is directed toward the eigenanalysis of open cavities, which will provide the means for physical insight and thus novel antenna designs, such as lens or cavity-backed structures.

2.4 FDFD Eigenanalysis of Periodic Waveguide Structures

The current work elaborates on the study of periodic structures loaded either with anisotropic or isotropic media. Although exploiting a previous frequency-domain finite-difference curved-waveguide approach (Section 2.2), these periodic structures must be modeled and discretized in a three-dimensional domain (Figure 4), or as a three-dimensional waveguide with periodic surfaces. This is necessary in order to allow an inhomogeneous unit cell not only across the cross section, but also along the propagation direction, as shown, for example, in Figure 5. An arbitrary unit cell in all three directions is hence considered (Figure 5), offering a general three-dimensional periodic waveguide analysis. The discretization of the three-dimensional unit cell is carried out in a manner similar to that described in Section 2.2 (a detailed analysis will be soon submitted for publication), but the operators involved in the two Maxwell curl equations are discretized over the whole solution domain with the aid of a three-dimensional Yee type of curvilinear grid (Figure 6).

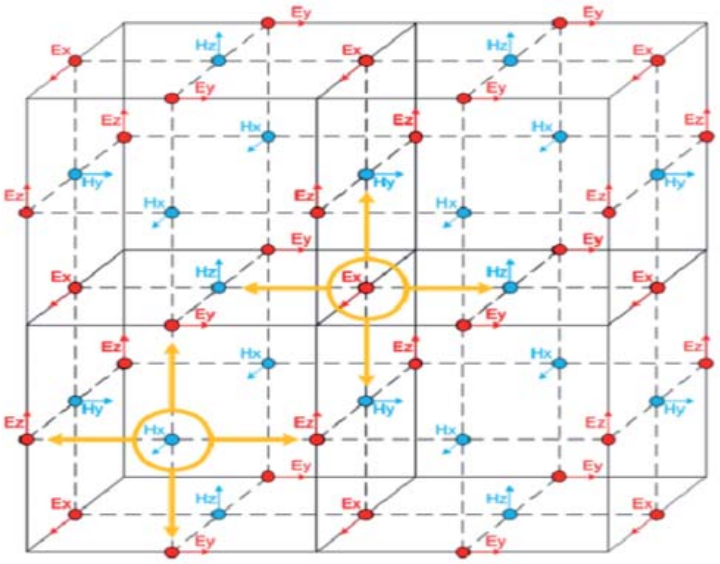

Figure 6. A three-dimensional rectangular Yee-type cell with E and H grids for the discretization of three-dimensional waveguides.

The final aim of this effort is the analysis of finite periodic structures based on a "Mode-Matching Rationale." First an eigenanalysis of "infinite periodic structures" will be carried out, in order to acquire the Floquet wavenumbers and the corresponding numerical eigenfunctions, exploiting the convenience of modeling just a single spatial period (unit cell). An eigenanalysis methodology is adopted using finite differences in the frequency domain (FDFD), in order to evaluate the Floquet wavenumbers. In turn, the electromagnetic field within the finite periodic section will be expanded as a superposition of all necessary (theoretically infinite) Floquet harmonics (eigenfunctions), similar to the expansion in a regular waveguide section. The finite periodic section will next be represented by a generalized scattering matrix, following a mode-matching scheme. Only the frequency-domain finite-difference eigenanalysis of infinite three-dimensional periodic waveguides will be presented herein. According to a detailed analysis in our previous work [4], an eigenvalue problem is formulated in the form

$$\mathrm{A}\vec{e} = \omega^2 \vec{e}\,, \tag{33}$$

where the A matrix is equal to

$$\mathrm{A} = E^{-1} R_m M^{-1} R_e\,. \tag{34}$$

E is the discretized permittivity tensor for the unit cell, and likewise M is the discretized permeability tensor. R_m is a matrix representing the discretized magnetic curl operator, while R_e is a matrix representing the discretized electric curl operator.

The periodicity of infinite structures can be modeled by two approaches. The first scheme adopts the usual periodic boundary conditions (PBCs) approach. The second scheme is inspired by the analytical studies of periodic structures mainly elaborated in the photonics regime, wherein the field components are represented from the beginning as a Floquet expansion with unknown coefficients. Our novel scheme stems from these analytical approaches, and is directed towards incorporating a Floquet field expansion within the frequency-domain finite-difference formulation. Both are based on the Floquet Theorem, which states that in a periodic system, for a given mode of propagation at a given steady-state frequency, the fields at one cross section differ from those one period (or an integer number of multiple periods) away by only a complex exponential constant [20].

2.4.1 Periodic Boundary Conditions Scheme

First, the modeling of an infinite periodic structure shown in Figure 4 is reduced to the model of a unit cell. Secondly, periodic boundary conditions (PBCs) are imposed on the periodic surfaces of the unit cell. Periodic boundary conditions are, in turn, applied to the two discretized curl equations of the electric and magnetic fields. Moreover, appropriate boundary conditions for the remaining surfaces – which are either perfect electric conductors (PECs) or perfect magnetic conductor (PMCs), and possibly perfect matching layers for open structures – are imposed on the previous matrices (R_e, R_m).

2.4.2 Incorporating the Floquet Field Expansion

A more-accurate simulation of infinite periodic structures is expected when the Floquet field expansion is incorporated into the frequency-domain finite-difference formulation. The Floquet Theorem is a discrete spatial Fourier transform (series), since the electric/magnetic field of lossless periodic structures is a spatial periodic function. The electric and magnetic field are hence expressed as

$$E_{(x,y,z)} = \sum_{n=-\infty}^{n=+\infty} C_{n_E} e^{-j\beta_n z}\,, \tag{35}$$

$$H_{(x,y,z)} = \sum_{n=-\infty}^{n=+\infty} C_{n_H} e^{-j\beta_n z}\,, \tag{36}$$

where $C_{n_{E,H}}$ are the unknown Floquet coefficients or the weighting factors of the expansion, expressed as

$$C_{n_E} = \frac{1}{p}\int_0^p E_{(x,y,z)} e^{j\beta_n z} dz\,, \tag{37}$$

$$C_{n_H} = \frac{1}{p}\int_0^p H_{(x,y,z)} e^{j\beta_n z} dz\,, \tag{38}$$

where β_n is the Floquet wavenumber, which is equal to

$$\beta_n = \beta_0 + \frac{2n\pi}{p}\,, \tag{39}$$

and n is the index of the Floquet spatial harmonics.

The evaluation of the integrals in Equations (37) and (38) requires an interpolation between the adjacent nodes of the electric and magnetic field, discretized according to

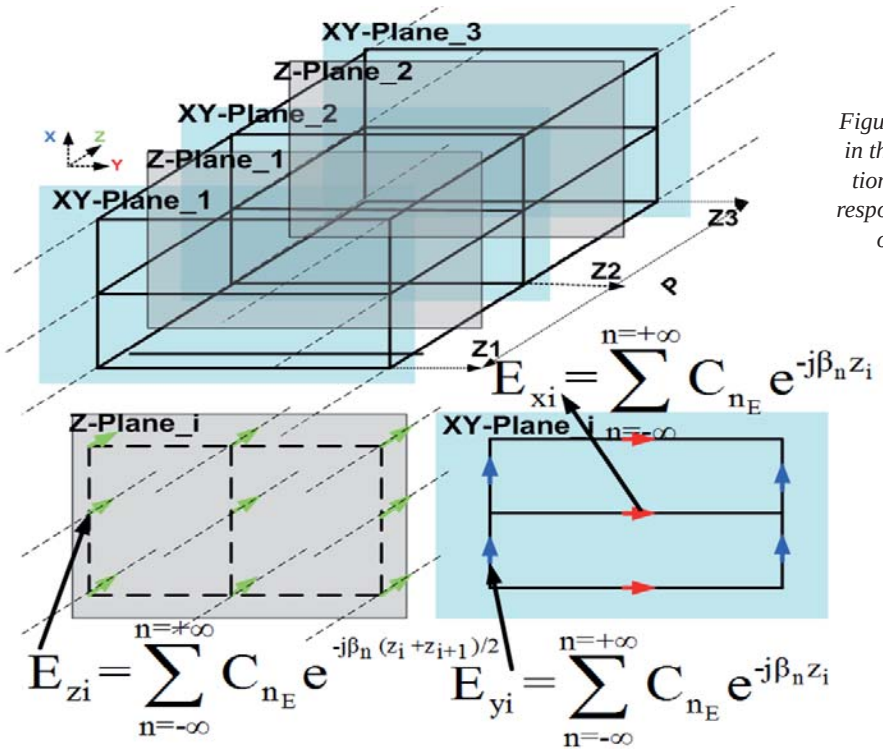

Figure 7. A unit cell with periodicity in the z direction. Linear interpolation was applied between the corresponding pairs of successive nodes of xy-Plane_i and z-Plane_i.

Yee's cell (Figure 6). Linear interpolation is applied only in the direction of the structure's periodicity, as depicted in Figure 7. The discretized Floquet coefficients are the same for either the electric or magnetic field. There are two types of Floquet coefficients, depending on the position of the electric/magnetic nodes according to the Yee cell (Figure 6). $C_{n_{XY}}$ is related to the nodes $(\mathrm{E}_x^i, \mathrm{E}_y^i)$ or $(\mathrm{H}_x^i, \mathrm{H}_y^i)$ that are placed in the *xy* plane, and C_{n_z} is related to the corresponding $(\mathrm{E}_z^i$ or $\mathrm{H}_z^i)$ nodes that are placed along *z* plane, as shown in Figure 6.

Analytically integrating the expressions in Equations (37) and (38), these coefficients read

$$C_{n\mathrm{E}_{XY}} = \frac{1}{p}\frac{e^{j\beta_n z_o}}{j\beta_n}\left(e^{j\beta_n \Delta z} - 1\right)\left\{\sum_{i=0}^{N-1}\left(\mathrm{E}_x^i - \frac{\mathrm{E}_y^i}{\Delta z}\frac{1}{j\beta_n}\right)e^{ji\beta_n \Delta z} + \sum_{i=0}^{N-1}\left[\mathrm{E}_y^i e^{j(i+1)\beta_n \Delta z}\right]\right\}, \quad (40a)$$

$$C_{n\mathrm{H}_{XY}} = \frac{1}{p}\frac{e^{j\beta_n z_o}}{j\beta_n}\left(e^{j\beta_n \Delta z} - 1\right)\left\{\sum_{i=0}^{N-1}\left(\mathrm{H}_x^i - \frac{\mathrm{H}_y^i}{\Delta z}\frac{1}{j\beta_n}\right)e^{ji\beta_n \Delta z} + \sum_{i=0}^{N-1}\left[\mathrm{H}_y^i e^{j(i+1)\beta_n \Delta z}\right]\right\}, \quad (40b)$$

$$C_{n\mathrm{Ez}} = \frac{1}{p}\sum_{t=0}^{\mathrm{N}}\left(\mathrm{E}_z^{i+1} e^{ji\beta_n \Delta z}\frac{e^{j\beta_n \Delta z} - 1}{j\beta_n}\right), \quad (41a)$$

$$C_{n\mathrm{Hz}} = \frac{1}{p}\sum_{t=0}^{\mathrm{N}}\left(\mathrm{H}_z^{i+1} e^{ji\beta_n \Delta z}\frac{e^{j\beta_n \Delta z} - 1}{j\beta_n}\right). \quad (41b)$$

2.4.3 Similarities to Bragg Diffraction

It is important to mention that the discretized Floquet coefficients via finite differences lead to Equations (40) and (41), which are similar to Bragg diffraction expressions. Considering a plane wave to impinge perpendicularly on a periodic structure, as shown in Figure 8, the total electric field is given according to the Bragg diffraction expressions as

$$E_{total} = E_{reflected} + E_{transmitted} \quad (42)$$

$$= \sum_{i=m+1}^{N}\left[E_{ri} T^{i\text{-}1}\,\mathrm{Re}^{-j(i-1)B\Lambda} + E_{in} T^{i}\,\mathrm{Re}^{-j(i-1)B\Lambda}\right]$$

where T^i is the transmission coefficient. The discretized component of the electric field (e.g., $\vec{\mathrm{A}_z}$) is described according to the frequency-domain finite-difference formulation as

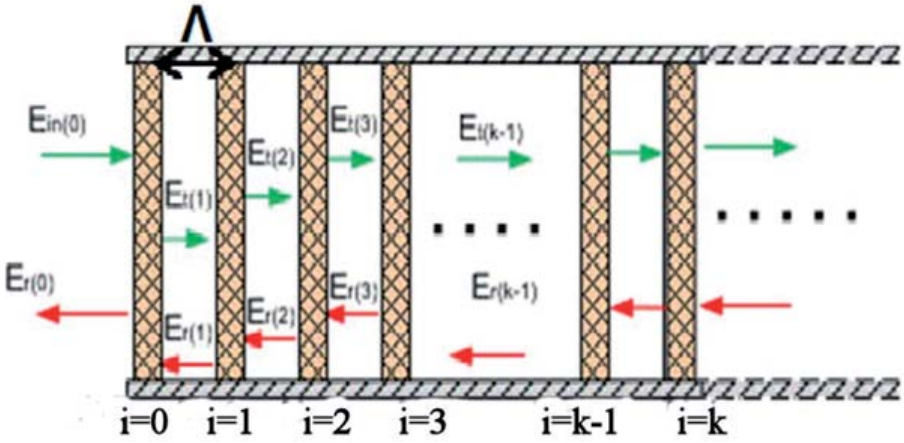

Figure 8. A plane-wave Bragg diffraction within a structure of alternating dielectric slabs of infinitesimal width.

$$\overrightarrow{E_z} = \sum_{n=-\infty}^{\infty} \frac{\left(e^{j\beta_n \Delta z} - 1\right)}{Z_p j\beta_n} \sum_{k=1}^{k} \left\{ \left[E_{zk} e^{j\,\beta n(k-1)\Delta z} \right] e^{-j\beta nz} \right\} \hat{z} \tag{43}$$

It is obvious that both the expressions in Equations (42) and (43) are superpositions of reflected and transmitted waves at each discontinuity (each point) of the periodic structure. This characteristic of the proposed method plays a vital role in offering physical insight for periodic structures that can support the so called frozen modes.

2.4.4 Future Extensions

The first priority of this effort was directed toward the solution of a β formulation eigenproblem that will provide the complex propagation constants of open and lossy structures. Currently, dispersion curves are obtained though a linear *w* formulation, and the main obstacle to move on is the inherent nonlinearity of the β formulation. Again, learning from analytical techniques utilized in canonical structures, we will try to reformulate this approach in order to yield a linear β formulation. Closely related to this extension is the elaboration on a scheme providing an exact unbounded domain truncation, since any known local truncation technique gives rise to fictitious eigenmodes (e.g., Berenger modes occurring when a perfectly matched layer is adopted). A global radiation condition based on the Dirichlet-to-Neumann formalism is planned. Finally, this work could be completed by a mode-matching scheme handling finite periodic structures.

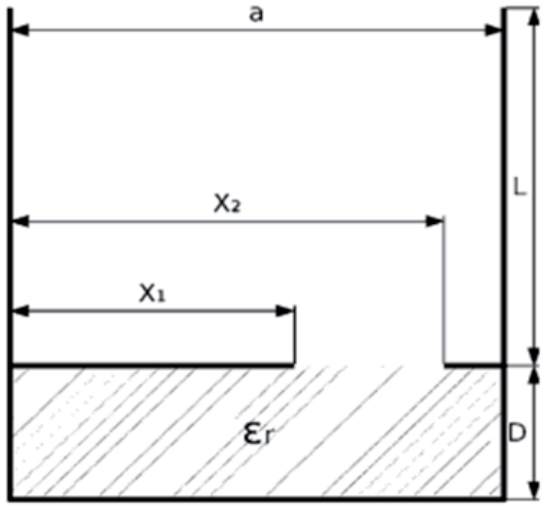

Figure 9. A laterally shielded slot line. The dielectric constant was $\varepsilon_r = 2.56$, and its dimensions were $\alpha = 2.2\,mm$, $D = 1.59\,mm$, $X_1 = 1\,mm$, and $X_2 = 2.1\,mm$.

3. Indicative Numerical Results and Discussions

Indicative results presenting the capabilities of the above methodologies are given next. Extensive validations and more complete representations can be found in the publications specific for each method, e.g., [1-4, 12-14].

3.1 The Hybrid Finite-Element Results

The first structure examined is the laterally shielded open-top slot line shown in Figure 9. Gomez-Tornero et al. [21] also analyzed this slot line, using their space-domain MoM. In Figure 10, the longitudinal propagation constant is plotted for different lengths (*L*) of the parallel-plate waveguide used to shield the structure. The frequency was 50 GHz. Very good agreement for both the phase (see Figure 10a) and the leakage (see Figure 10b) constants was observed. At this point, it is worth mentioning that in both cases, *the approximate linear formulation performed unexpectedly well*. In fact, it could be exploited as a fast tool for the design of leaky- and surface-wave structures. In turn, the nonlinear formulation can serve as a fine-tuning (trimming) tool.

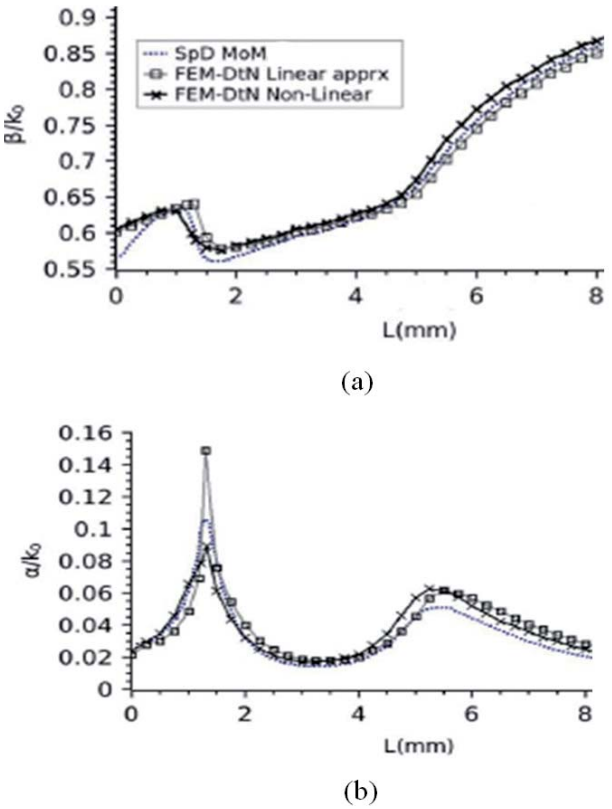

Figure 10. The normalized longitudinal propagation constant of the slot line of Figure 9 (space domain MoM: SpD MoM; finite-element Dirichlet-to-Neumann method: FEM-DtN): (a) The phase constant; (b) The leakage constant.

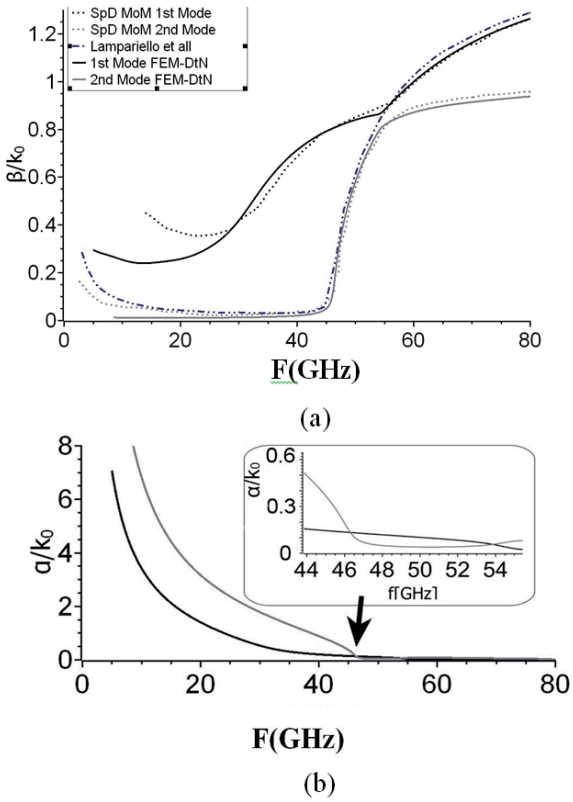

Figure 11. The normalized longitudinal propagation constant of the leaky-wave antenna of Figure 9 (space domain MoM: SpD MoM; finite-element Dirichlet-to-Newmann method: FEM-DtN): (a) The phase constant; (b) The leakage constant. The horizontal axis is the frequency in GHz for both plots.

The second example again deals with the laterally shielded slot line of Figure 9, but now the length of the parallel-plate waveguide shielding was fixed at $L = 2$ mm, and the longitudinal propagation constant is plotted as a function of frequency. The dispersion characteristics of this structure were also studied in [21] and [22], but the authors therein presented only the longitudinal phase constant (β/k_0), and no results for the leakage constant were given.

The complete dispersion characteristics were evaluated herein, and are depicted in Figure 11. For the phase constant, good agreement was observed when the current results were compared against those of [21]. At frequencies below 25 GHz, some discrepancies between the results provided by the finite-element Dirichlet-to-Neumann method and [21] were observed. The finite-element Dirichlet-to-Neumann method managed to predict the coupling phenomena between the "channel guide" (labeled "1st mode") and the desired leaky mode (labeled "2nd mode"). The coupling occurred at $f \approx 46$ GHz, where both the attenuation (α) and phase (β) constants of the two modes were equal, namely, their dispersion curves intersected at the same frequency. For more details on the coupling phenomena, refer to [2, 18], and for a more general explanation see [23]. The results provided by [22] referred to a structure with an infinite lateral shielding. This is the reason why there was no "channel-guide" mode present, and thus no coupling phenomena occurred in the results provided by [21]. Using the present FEM Dirichlet-to-Neumann method, we were able to reveal a novel mode-coupling phenomenon. This coupling occurs between the dominant mode of a microstrip line and a leaky mode created by the field scattered at the edges of its finite substrate. Preliminary results were presented in the conference paper [24], while detailed work is under preparation.

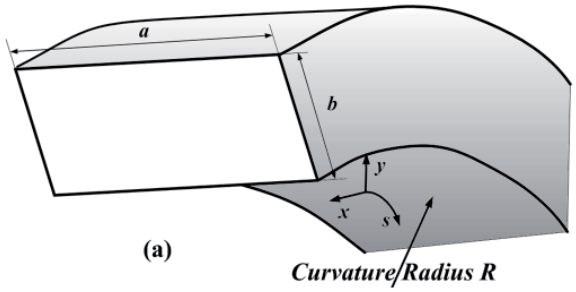

Figure 12. An empty rectangular X-band waveguide ($a = 22.86$ mm, $b = 10.16$ mm), curved downwards: $R = 0.02$ m, $R/b = 2$.

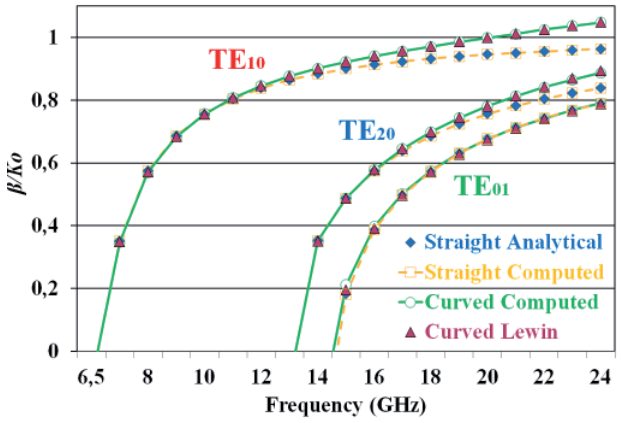

(a)

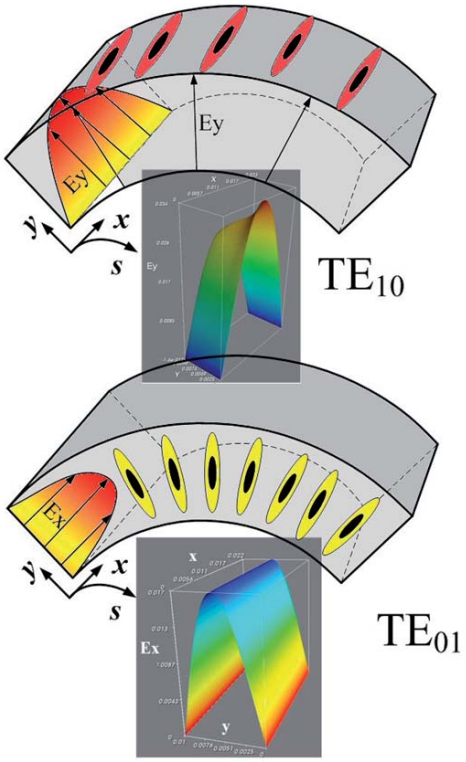

(b)

Figure 13. The results for the curved rectangular waveguide of Figure 12: (a) The dispersion curves of a curved and straight WR-90 rectangular waveguide (downward curvature). (b) The electric-field distributions for the TE_{10} *and* TE_{01} *modes.*

3.2 The Curvilinear FDFD Method Results

The first example refers to an empty rectangular waveguide, curved downwards (the same behavior occurs when curved upward, due to the waveguide's symmetry) as shown in Figure 12 [2].

The dispersion curves shown in Figure 13a correspond to the first three modes, TE_{10} , TE_{20} , and TE_{01} , computed for both curved waveguides and for a straight waveguide of the same cross section.

The propagation constants for the straight waveguide were compared with the corresponding analytical solutions. On the other hand, the propagation constants for the curved waveguides were compared with Lewin's perturbation theory [15]. This theory dealt with curvature effects in simple canonical waveguide geometries. Particularly, for the case of an empty curved rectangular waveguide, the propagation-constant correction formulas were given either for the dominant or for the higher-order transverse electric (TE) modes, [2, 15], either for vertical or for sideways curvature.

As explained by Lewin and also shown in Figure 13a, a remarkable change in the propagation constants was observed when the waveguide was curved. This change depended on the particular mode, the structure's dimensions, the curvature radius, the curvature direction, and the operating frequency. In particular, a downward curvature led to a continuous increase (shifted upward) for the TE_{10} and TE_{20} modes. These curvature effects started after a specific frequency (interchange frequency), depending on the dimensions of the waveguide, e.g., at 8.8 GHz for the TE_{10} mode (Figure 13b). For lower frequencies, the dispersion curves were shifted downward by a smaller amount. In parallel, the third mode (TE_{01}) remained almost unaffected. This was also observed in Figure 13b, where the electric field's distributions for the TE_{10} and TE_{01} modes are shown. It was clearly observed that when the curvature radius was parallel to the electric field's vector (TE_{10} case), there was a significant distortion in the electric field's distribution. As shown in Figure 14, this distortion

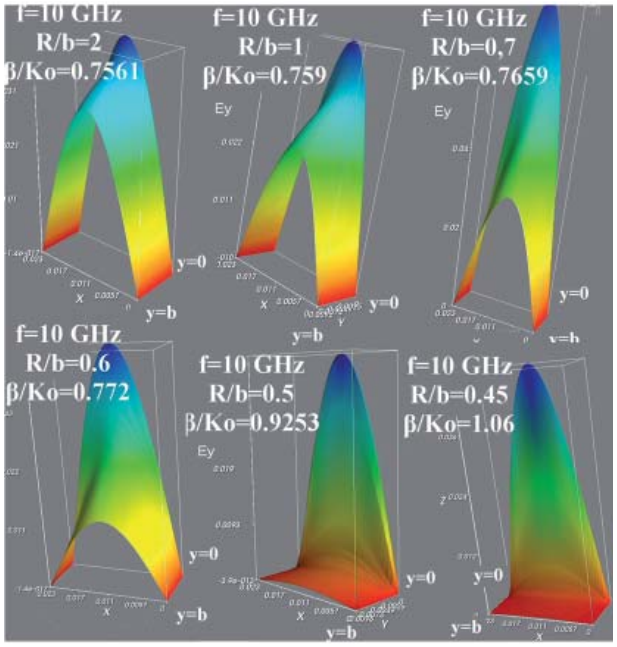

Figure 14. The electric-field distributions for the TE_{10} *mode for the curved rectangular waveguide of Figure 12, for different curvature ratios.*

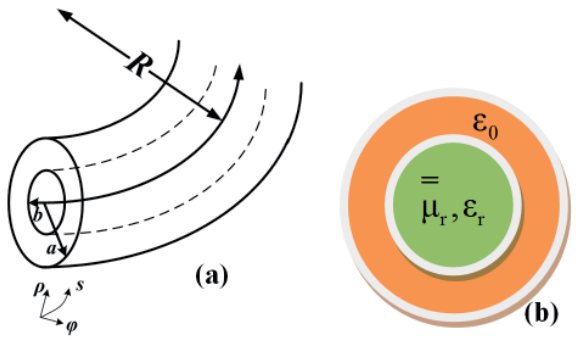

Figure 15. A curved circular waveguide with a longitudinally concentric ferrite rod ($R/2a = 1.5$).

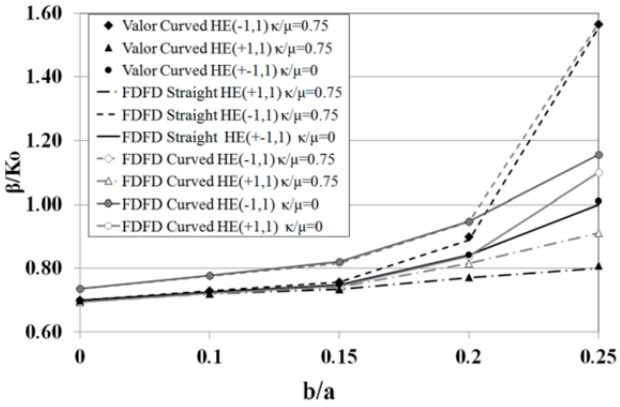

Figure 16. The normalized phase constants for the ferrite-loaded curved circular waveguide of Figure 15, compared with those for the corresponding straight waveguide (FDFD method and Valor [25]).

got worse for higher curvatures (smaller curvature radius). After some critical point, the whole propagation approach broke (Figure 14, ratio $R/b = 4.5$). On the other hand, when the curvature radius was normal to the electric field's vector (TE_{01} case), a negligible distortion in the electric field's distribution was observed.

The second example deals with a curved circular waveguide involving a longitudinally concentric ferrite rod, as shown in Figure 15 [14]. This example aimed at demonstrating the abilities of the method to handle anisotropic media such as magnetized ferrites, along with a curvilinear mesh. In this case, the permeability tensor was expressed as

$$\bar{\bar{\mu}} = \begin{bmatrix} \mu & -j\kappa & 0 \\ j\kappa & \mu & 0 \\ 0 & 0 & 1 \end{bmatrix}. \qquad (44)$$

Initially, the straight case shown in Figure 15b was simulated, and the results were compared with those given by Valor [25], which were almost identical. The discretization adopted a pure circular cylindrical grid. The normalized phase constants were extracted as a function of the ratio b/a for the dominant $\mathrm{HE}(1,1)$ mode, with κ/μ as a parameter. As shown, when $\kappa/\mu = 0$, the ferrite rod was simplified to a transverse diamagnetic rod where all left- and right-hand circularly polarized modes were degenerated, as analyzed in our previous work [2, 14]. Left- and right-hand circularly polarized $\mathrm{HE}(\pm 1,1)$ modes thus had the same dispersion curves. On the other hand, when $\kappa/\mu \neq 0$, a degeneration removal phenomenon appeared (known as birefringence [26]), and the $\mathrm{HE}(+1,1)$ and $\mathrm{HE}(-1,1)$ dispersion curves were separated. The computed results for that case (black lines) were almost identical to those obtained by Valor (black triangles, diamonds, and circles) [25], following

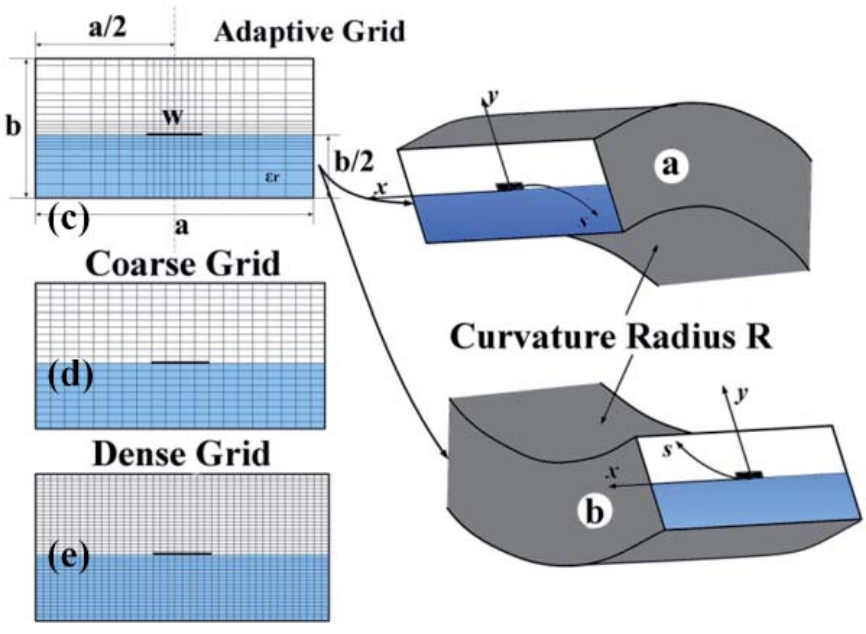

Figure 17. A curved shielded microstrip line: (a) downwards; (b) upwards ($a = 8$ mm, $b = 4$ mm, $w = 2$ mm, $\varepsilon_r = 3.3$, curvature radius $R = 9.5$ mm); (c) Adaptive grid; (d) Coarse grid; (e) Dense grid.

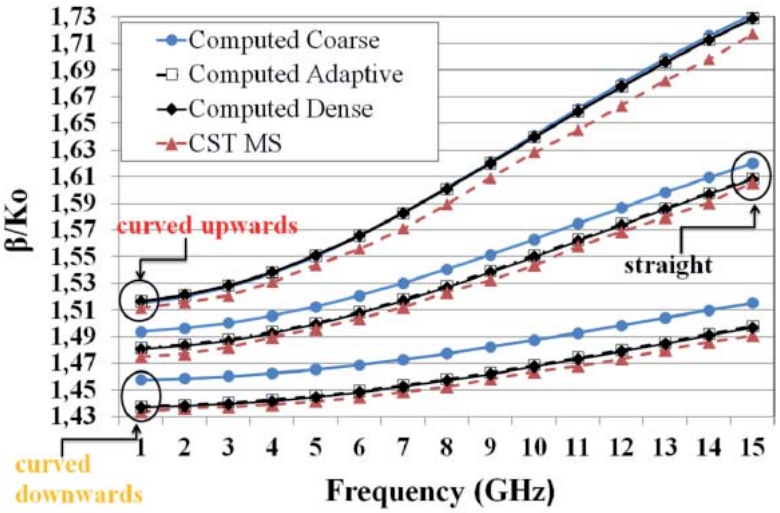

Figure 18. The normalized dispersion curves of the dominant mode of the curved microstrip lines of Figure 10, compared against those of the corresponding straight line.

exactly the above theory. In particular, the degeneration removal occurred up to 50% at a ratio equal to $b/a = 2.5$.

After the above validation, the curved waveguide structure shown in Figure 15a was exclusively analyzed with the curvilinear frequency-domain finite-difference method. The waveguide curvature led to some important results, as shown in Figure 16. For the $\kappa/\mu = 0$ case, a significant (up to 15% at a ratio of 2.5) degeneration removal occurred (two grey continuous lines above the continuous black line in Figure 16), as was expected due to the waveguide's curvature [2, 14]. On the other hand, for $\kappa/\mu \neq 0$, an important increase in the eigenvalues (phase constants) for both the $\mathrm{HE}(+1,1)$ and $\mathrm{HE}(-1,1)$ modes occurred. This increase rose up to 9% for the $\mathrm{HE}(+1,1)$ mode at a ratio equal to 2.5, and 6% for the $\mathrm{HE}(-1,1)$ mode at a ratio equal to 2.

A third case elaborated on the "adaptive grid" and considered a shielded rectangular microstrip line curved in two different directions, as shown in Figure 17. The normalized phase constants for the dominant quasi-TEM mode, compared to those of the corresponding straight line, are presented in Figure 18. For each case, the three different grids shown in Figure 17 were used. Initially, the examined geometry was analyzed using a coarse uniform mesh of $20 \times 20 = 400$ cells (Figure 17d). Afterwards, the number of uniform cells was increased to $40 \times 40 = 1600$ (Figure 17e). Finally, the adaptive grid of Figure 17c, with 400 nonuniform cells, was utilized. It proved to provide the same accuracy as the uniform grid with 1600 cells.

In order to validate these results, the commercially available electromagnetic simulator *Microwave Studio* [27] was employed. Note that commercially available electromagnetic simulators do not support the eigen-analysis of curved waveguides. Also, for the straight case, a three-dimensional model was adopted, and the eigenvalues were extracted through an ABCD transformation to S_{21} ,including a phase unwrapping. When the waveguide was curved upwards, an increase in the normalized phase constants compared to the straight guide was observed, as shown in Figure 18. That increase rose to 7.5% for the studied case, where the ratio between the curvature's radius and the vertical waveguide's dimension was equal to 1.1875. To the contrary, a downwards curvature yielded a decrease up to 7% in the normalized phase constants with respect to the straight waveguide. The deviation between the computed results and those extracted from the electromagnetic simulator [27] were less than 0.78% for the dense grid and the adaptive grid, while for the coarse grid, the deviation rose to 1.8%.

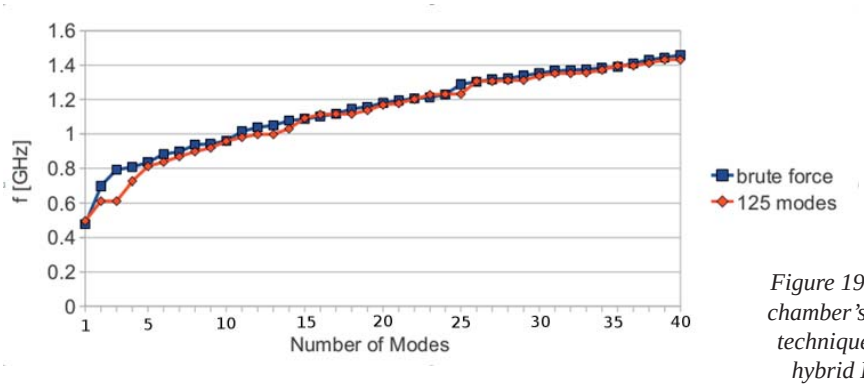

Figure 19. A comparison of a reverberation chamber's resonant frequencies: brute-force technique (squared line) and the proposed hybrid DDM technique (diamond line).

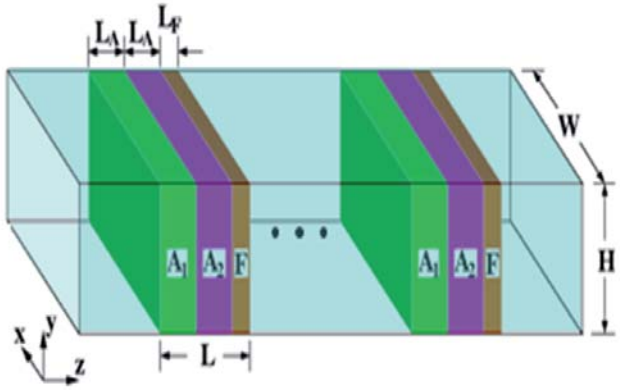

Figure 20. A periodic waveguide structure loaded with two misaligned anisotropic dielectric media (A_1 , A_2) and one gyrotropic Ferrite (F).

It was obvious that the adaptive grid saved computer resources while retaining the required accuracy. Thus, the frequency-domain finite-difference method indeed shares the Finite-Element Method's convenience in the discretization, but the frequency-domain finite difference has the additional advantage of readily accounting for any material complexity or anisotropy. A further extension to more-advanced adaptive grids is necessary (beyond the simple nonuniform grid of Figure 17e) to cope with complex geometries.

3.3 Hybrid DDM and Truncation Eigenanalysis

A reverberation chamber (RC) (0.2 m × 0.4 m × 0.5 m) with metallic walls was loaded with two perturbations (the mode-stirrer's area and the area of the equipment under test, EUT). In Figure 19, a comparison of the resonant frequencies obtained using a brute-force method and the proposed hybrid domain-decomposition method (DDM) formulation is shown. For the computation of the eigenfrequencies, a fictitious box (0.16 m × 0.3 m × 0.35 m) was considered, discretized with a mesh of 1000 tetrahedral elements. The volume of the fictitious area was large enough to totally enclose the two perturbations, but in any case smaller than the original structure (only 42% of the geometry was discretized). For the area outside the fictitious box, an eigenfunction expansion of 125 modes was considered. The whole simulation procedure required five minutes from the initialization of the geometry to the exportation of the eigenvalues. For the case of the brute-force technique, a mesh of 5000 elements was required for the same accuracy, while the simulation procedure needed almost 5.5 minutes. Even if the time duration between the two techniques was not so different, there was a significant difference in the memory requirements. For the brute-force technique, 113.67 MB was used in comparison to the hybrid technique, which required only 5.79 MB. The main part of the CPU time required by the hybrid DDM method was spend on calculating certain types of coupling integrals. However, it is possible to speed up their evaluation with the aid of well-established techniques. This constitutes one of our next tasks.

3.4 FDFD Periodic Structures Eigenanalysis

The strength of the present method was actually revealed when a very demanding periodic structure, as shown in Figure 20, was simulated. The major difficulty stemmed from the very thin ferrite media, for which adaptive meshing (very dense inside and at the ferrite interface) was employed in order to capture the desired accuracy. The same structure was analyzed by Chilton et al. [28]. The electric and magnetic permittivity and permeability tensors for the corresponding layer of the periodic structure shown in Figure 20 were as follows:

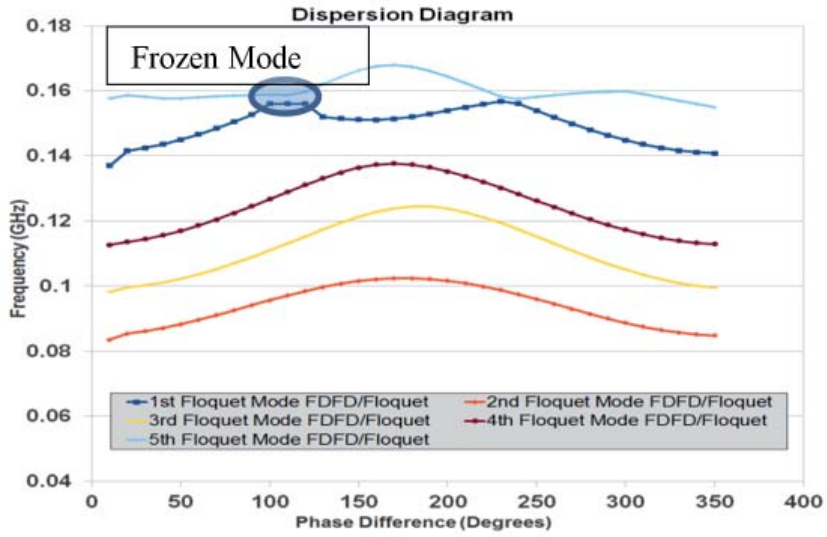

Figure 21. A dispersion diagram for the geometry shown in Figure 20. The TE_{20} mode is identified as a frozen mode.

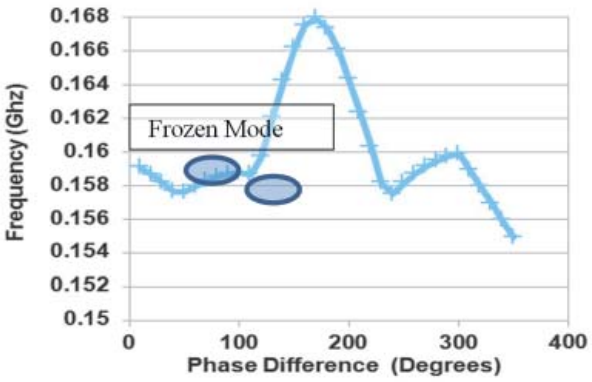

Figure 22. A closer look (zoom in) of the frozen-mode dispersion curve given in Figure 21.

$$\bar{\bar{\varepsilon}}_{A1} = \begin{bmatrix} 28.47 & 0 & -15.14 \\ 0 & 1.0 & 0 \\ -15.14 & 0 & 10.99 \end{bmatrix},$$

$$\bar{\bar{\varepsilon}}_{A2} = \begin{bmatrix} 28.47 & 0 & 15.14 \\ 0 & 1.0 & 0 \\ -15.14 & 0 & 10.99 \end{bmatrix},$$

$$\bar{\bar{\mu}}_{F} = \begin{bmatrix} 31.48 & 0 & 28.52\,j \\ 0 & 1.0 & 0 \\ 28.52\,j & 0 & 31.48 \end{bmatrix},$$

$$\mu_{A1} = \mu_0 , \qquad (45)$$

$$\mu_{A2} = \mu_0 ,$$

$$\varepsilon_f = 5.4 .$$

The solutions of the eigenvalue problem of Equation (33) produced the dispersion diagram shown in Figure 21. It was obvious that unlike the rest of the curves, the sixth curve of the dispersion diagram was not symmetrical with respect to 180°, due to the anisotropic layers of the periodic structure. A careful observation revealed that the sixth curve, corresponding to the TE_{20} mode, was parallel to the normalized propagation constant axis in the neighborhood of 100°. This meant that the group velocity tended to zero (Figure 22) for the specific Floquet wavenumber, creating the so-called frozen mode. Most of electric field's energy had been encapsulated into the last narrow anisotropic layer (F), as shown in Figure 23, due to the zero group velocity. This in turn led to a rapid increase in the field's intensity.

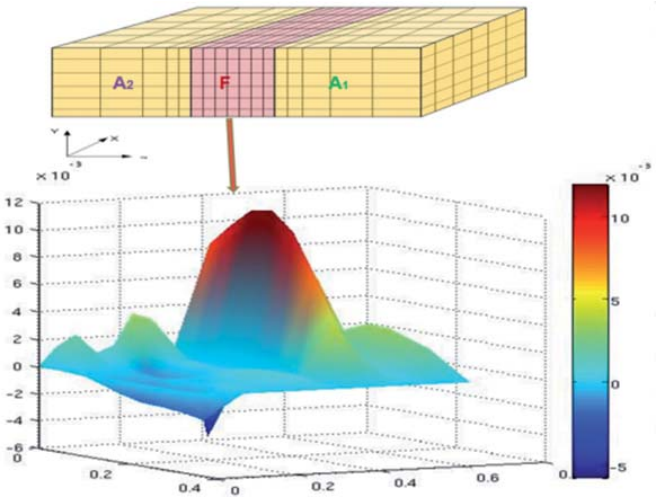

Figure 23. The correspondence between the discretized periodic structure using an adaptive mesh with the magnitude of the electric field.

4. Conclusions

A review of the effort on the eigenanalysis of two-dimensional arbitrarily shaped, loaded or curved as well as closed, three-dimensional electrically large waveguide structures was presented. The strengths as well as the limitations of the elaborated methodologies were identified. Indicative numerical examples showed the capabilities of these methodologies in the study of arbitrary waveguides, such as open radiating straight anisotropically loaded waveguides, as well as waveguides periodically loaded with anisotropic media, even when frozen modes were supported. The corresponding improvements put forward referred to minimizing the computational cost of exact global Dirichlet-to-Neumann domain-truncation methods, and extending the work to radiating periodic waveguides. The eigenanalysis of three-dimensional structures is at its first steps, and only closed but electrically large structures have already been studied. The extension towards open three-dimensional geometries, including characteristic-mode eigenanalysis, constitutes one of our priorities.

5. Acknowledgment

This work was financially supported by the Greek Ministry of Education, Lifelong Learning and Religious Affairs through the research project THALIS Design Techniques for Digitally Controlled RF-Microwave Structures Appropriate for Software Defined – Cognitive Radio (RF-EIGEN-SDR).

6. References

1. P. C. Allilomes and G. A. Kyriacou, "A Nonlinear Finite-Element Leaky-Waveguide Solver," *IEEE Transactions on Microwave Theory and Techniques*, **55**, 7, July 2007, pp. 1496-1510.

2. C. S. Lavranos and G. A. Kyriacou, "Eigenvalue Analysis of Curved Waveguides Employing an Orthogonal Curvilinear Frequency Domain Finite Difference Method," *IEEE Transactions on Microwave Theory and Techniques*, **57**, 3, April 2009, pp. 594-611.

3. C. L. Zekios, P. C. Allilomes and G. A. Kyriacou. "Eigenfunction Expansion for the Analysis of Closed Cavities," 2010 Loughborough Antennas and Propagation Conference, November 2010, pp. 537-540.

4. C. L. Zekios, P. C. Allilomes and G. A. Kyriacou, "On the Evaluation of Eigenmodes Quality Factor of Large Complex Cavities Based on a PEC Linear Finite Element Formulation," *IET Electronics Letters*, **48**, 22, October 2012, pp. 1399-1401.

5. S. Lavdas, Ch. Lavranos, and G. A. Kyriacou, "Periodic Structures Eigenanalysis Incorporating the Floquet Field Expansion," ICEAA IEEE APWC Conference, Turin, Italy, September 2011.

6. J. D. Jackson, *Classical Electrodynamics, Third Edition*, New York, Wiley, 1999, p. 431.

7. D. M. Pozar, *Microwave Engineering, Second Edition*, New York, Wiley, 1998, p. 133.

8. C. Reddy, M. Deshpande, C. Cockrell, and F. Beck, "Finite Elements Method for Eigenvalue Problems in Electromagnetics," NASA Langley Research Center, Hampton, VA, Tech. Rep. 3485, December 1994.

9. R. F. Harrington, "Boundary Integral Formulations for Homogeneous Material Bodies," *J. Electromagnetic Waves and Applications*, **3**, 1, 1989, pp.1-15.

10. P. Hager, *Eigenfrequency Analysis: FE-Adaptivity and Nonlinear Eigen-Problem Algorithm*, PhD dissertation, Department of Structural Mechanics, Chalmers University of Technology, Göteborg, Sweden, 2001.

11. R. Lehoucq, K. Maschhoff, and D. Sorensen, ARPACK homepage, available at http:// www.caam.rice.edu/software/ARPACK/.

12. C. S. Lavranos and G. A. Kyriacou, "Eigenvalue Analysis of Curved Waveguides Employing FDFD Method in Orthogonal Curvilinear Co-ordinates," *Electronic Letters*, **42**, 12, June 2006, pp. 702-704.

13. C. S. Lavranos, D. G. Drogoudis, and G. A. Kyriacou, "Eigenvalue Analysis of Waveguides and Planar Transmission Lines Loaded with Full Tensor Anisotropic Materials," *PIERS Online*, **5**, 5, 2009, pp. 471-475.

14. C. S. Lavranos, S. Lavdas and G. A. Kyriacou, "Eigenvalue Analysis of Planar or Curved Shielded or Open Transmission Lines Loaded with Full Tensor Anisotropic Materials," ICEAA IEEE APWC Conference, Turin, Italy, September 2011.

15. L. Lewin, D. C. Chang, and E. F. Kuester, *Electromagnetic Waves and Curved Structures*, London, Peregrinus, 1977.

16. D. C. Sorensen, "Implicit Application of Polynomial Filters in a K-Step Arnoldi Method," *SIAM Journal of Matrix Analysis and Applications*, **13**, 1, January 1992, pp. 357-385.

17. A. C. Cangellaris and R. Lee, "The By-Moment Method for Two-Dimensional Electromagnetic Scattering," *IEEE Transactions on Antennas and Propagation*, **AP-38**, September 1990, pp. 1429-1437.

18. T. H. Lehman, "A Statistical Theory of Electromagnetic Fields in Complex Cavities," Interaction Note 494, Sandia Labs, May 1993.

19. C. L. Zekios, "Study and Design of Reverberation Chambers Using Eigenanalysis," MSc thesis, Democritus University of Thrace, Polytechnic School, Department of Electrical and Computer Engineering, Xanthi, Greece, 2011.

20. Keqian Zhang and Dejie Li, *Electromagnetic Theory for Microwaves and Optoelectronics, Second Edition*, New York, Springer, 1998.

21. J. L. Gomez-Tornero, F. D. Quesada-Pereira, and A. Alvarez-Melcon, "A Full-Wave Space-Domain Method for the Analysis of Leaky-Wave Modes in Multilayered Planar Open Parallel-Plate Waveguides," *Int. J. RF Microw. Comput.-Aided Eng.*, **15**, 1, December 2005, pp. 128-139.

22. P. Lampariello, F. Frezza, and A. A. Oliner, "The Transition Region Between Bound-Wave and Leaky-Wave Ranges for a Partially Dielectric Loaded Open Guiding Structure," *IEEE Transactions on Microwave Theory and Techniques*, **38**, 12, December 1990, pp. 1831-1836.

23. H. Shigesawa, M. Tsuji, P. Lampariello, F. Frezza, and A. A. Oliner, "Coupling Between Different Leaky-Mode Types in Stub-Loaded Leaky Waveguides," *IEEE Transactions on Microwave Theory and Techniques*, **42**, 8, August 1994, pp. 1548-1560.

24. P. C. Allilomes, C. L. Zekios, A. N. Stafyllidis and G. A. Kyriacou, "A Novel Leaky Mode and Mode Coupling Effects Occurring in Finite Substrate Microstrip Lines and Patch Antennas," International Conference on Electromagnetics in Advanced Applications, ICEAA-IEEE APWC, Torino Italy, September 12-16, 2011, pp. 1257-1260.

25. L. Valor and J. Zapata, "Efficient Finite Element Analysis of Waveguides with Lossy Inhomogeneous Anisotropic Materials Characterized by Arbitrary Permittivity and Permeability Tensors," *IEEE Transactions on Microwave Theory and Techniques*, **43**, 10, 1995, pp. 2452-2459.

26. J. A. Kong, *Electromagnetic Wave Theory*, EMW Publishing, USA, 2005.

27 CST Microwave Studio Electromagnetic Simulator. CST, Framingham, MA, 1998-2003, available at: http://www.cst.com.

28. Ryan A. Chilton, Kyung-Young Jung, Robert Lee, and Fernado L. Teixeira, "Frozen Modes in Parallel-Plate Waveguides with Magnetic Photonic Crystals," *IEEE Transactions on Microwave Theory and Techniques*, **55**, 12, December 2007.

1 Note that detailed expressions are omitted, but they were explicitly given in Zekios' Master's thesis, available online in Greek [19].

Radio-Frequency Radiation Safety and Health

James C. Lin

Reassessing Exposure Safety Requirements for Mobile Phones

The CTIA, an organization representing the wireless communications industry, stated in a news release [1] that "CTIA welcomes the Federal Communications Commission's (FCC) continued careful oversight of this issue," with respect to the FCC's response to the US Government Accountability Office (GAO) report on mobile-phone safety [2]. The GAO recommended that the FCC reassess and, if appropriate, change its current RF exposure safety rules. The GAO also mentioned that the FCC is working on a draft document that has the potential of addressing the GAO's recommendations.

The GAO's report was issued following a year-long investigation into the adequacy of the FCC's rules. The investigation was requested by Reps. Edward J. Markey (D-MA), Henry Waxman (D-CA) and Anna Eshoo (D-CA). They are members of the House Energy and Commerce Committee, which has oversight authority over the FCC and the telecommunications industry.

The Environmental Working Group (EWG) applauded the three members of the US Congress for prompting the GAO investigation [3]. The EWG commended the GAO for the report demonstrating "the need for the FCC to review its cell phone safety standards" and expects "FCC will use the GAO's findings to update its safety standards for wireless devices."

For a change, at first glance both the environmental group and the wireless industry seem to be on the same page.

Given the Environmental Working Group's recommendation of "simple steps that cell phone users can take to decrease their exposure, such as using a headset and texting rather than talking," it is not a stretch to surmise that the EWG's most-favored outcome would be an FCC review that would lead to a substantial reduction of the current mobile-phone exposure limits.

On the other hand, the wireless industry's enchantment with the GAO report or the prospect of FCC reviewing its rules on radiation exposure from mobile phones may actually be pointed in the opposite direction, if past foretells the future. For instance, when the safety limits for localized exposure were relaxed by a factor of two or more in the 2006 IEEE "Standard for Safety Levels with Respect to Human Exposure to Radio Frequency Electromagnetic Fields," the Mobile Manufacturing Forum (MMF) was thrilled, notwithstanding that the pinnae (external human ears) was separated out from the rest of the head by this IEEE operation [4]. I will come back to the relaxed limits in due course.

The GAO report [2] indicated that the "FCC RF energy exposure limit may not reflect the latest research," since the FCC set the RF energy exposure limit for mobile phones in 1996, "based on recommendations from federal health and safety agencies and international organizations." One of the international organizations, namely, the IEEE, "updated its exposure limit recommendation, based on new research," in 2006. This new recommended limit allows for more RF exposure (by a factor of two or more).

The GAO report was the result of a year-long effort, during which its staff reviewed scientific research and interviewed experts in fields such as public health and engineering, officials from federal agencies, and representatives of academic institutions and consumer groups. To the best of my knowledge, the staff report was not circulated for comment by the interviewed experts.

It is fair to note that the 2006 update of the IEEE exposure standard was mostly an endeavor to harmonize with the existing International Commission on Nonionizing Radiation Protection (ICNIRP) guidelines, published in 1998 [5]. To be sure, the 2006 IEEE standard departs in major ways from its prior edition. One thing it did not do is to reduce the exposure limit. This column will focus on some of the more salient aspects applicable to cellular mobile communication.

In the frequency range of 100 kHz to 3 GHz, the new IEEE standard specific energy absorption rate (SAR)

James C. Lin is with the University of Illinois at Chicago, 851 S Morgan Street, M/C 154, Chicago, IL 60607-7053, USA; E-mail: lin@uic.edu.

(A version of this column appeared in *IEEE Antennas and Propagation Magazine*, **55**, 1, February 2013, pp. 218-220;

for localized exposure is 2.0 W/kg. This is the same as the ICNIRP (the FCC value is 1.6 W/kg) for most parts of the extremities (arms and legs distal from the elbows and knees, respectively, including the fingers, toes, hands, and feet). The IEEE basic restriction expressed in terms of SAR is 4.0 W/kg (the FCC value is 1.6 W/kg). The value of SAR is obtained by averaging over any 10 g of tissue, defined as a volume in the shape of a cube (the FCC averaging mass is 1 g).

Moreover, the new IEEE standard introduced an exclusion for the pinnae or the external ears by relaxation of the above-mentioned basic SAR restriction from 2 W/kg to 4 W/kg. In effect, for its purposes the IEEE standard formally declared that the pinnae is the same as are the extremities (arms, legs, fingers, toes, hands and feet). This decision separated out tissues in the pinnae, and severed the ear from the rest of the human head. The allowable SAR for other tissues in the head is 2 W/kg. Could this be a concession to the mobile-phone industry? Under operating conditions, where the mobile phone is positioned next to the head, SAR is the highest in the tissues of the pinnae.

Of equal if not more significance is the basic restriction for localized exposure at 2 W/kg in terms of SAR averaged over an increased mass of 10 g of tissue. The SAR value has been increased from 1.6 W/kg averaged over any 1 g of tissue to 2 W/kg over any 10 g of tissue. Aside from the numerical difference between the SARs (1.6 to 2.0), the volume of tissue mass used to define the SARs in the new IEEE standard was increased from 1 g to 10 g. The increase in tissue mass can have a profound influence on the actual quantity of RF energy allowed to be deposited in tissue by the new exposure standard. It has been well established that the distribution of absorbed microwave energy is nonuniform, and it varies greatly from point-to-point, tissue-to-tissue inside a body. An averaging volume that is as large as 10 g would tend to flatten the SAR distribution, whether it is computed or measured. The smoothing tends to artificially reduce the resulting SAR value. A 10 g SAR at 2 W/kg would thus be equivalent to 1 g SARs of 5 W/kg or higher. Simply put, the absorbed energy averaged over a defined tissue mass of 10 g is inherently low, compared to a 1 g SAR.

The answer to the question of whether the updated exposure limits promulgated by the new IEEE recommendation are based on new research is a qualified "No," for several reasons. The increase in allowable SAR values from 1.6 W/kg averaged over any 1 g of tissue to 2 W/kg over any 10 g of tissue in the new IEEE standard actually conformed to an older set of ICNIRP guidelines. The choice of averaging SAR over a tissue mass of 10 g instead of 1 g is regressive, in that it is less accurate and ignores progress made in the past couple of decades in the computational and experimental determination of SAR. The previous use of a 10 g mass was necessitated by the then-available gross spheroid body models, instead of the currently widely available detailed anatomical models, with precisions considerably greater than 1 g of tissue.

The close attention to mobile-phone exposure, and the wide availability of precision computational determinations of SAR in anatomical models, have revealed the pinnae as a site of high SAR for a mobile phone that is used next to the head, which is a new finding. However, the new IEEE standard elected to deal with it in other (rather bizarre) ways. As an example, at 2.5 GHz, the RF field-penetration depth in muscle tissue for a flat region is about 1.7 cm. A linear dimension of approximately 2.15 cm in the shape of a cube would be needed to make up 10 g of muscle tissue. Clearly, the exponentially attenuated SAR would be significantly greater close to (and more concentrated in) the superficial layer of muscle tissue, which would be easily revealed by the 1 g SAR, but masked by a 10 g SAR.

It should be noted that the sensitivity and resolution of present-day computational algorithms and resources, and experimental measurement schemes, can provide accurate SAR values with a spatial resolution on the order of 1 mm or less in dimension. The 1 g SAR is also scientifically a more-precise representation of localized RF or microwave energy absorption, and a more biologically significant measure of SAR distribution inside the body or head, than a 10 g SAR.

Only time will tell what the FCC may possibly do, or whether or not going forward it will change its current RF exposure safety rules. If the FCC does decide to change its current RF exposure safety rules, it would do well to note that since 1998, the scientific progress made in computational dosimetry has been exceptional. Instead of the homogeneous geometrical models of human and animal bodies, most if not all computational studies are based on heterogeneous, realistic anatomical models, using voxels of 1.0 mm or better resolution in biological tissues. To acknowledge this scientific achievement, the averaging volume has been changed to a volume of 2 mm × 2 mm × 2 mm for induced electric field and local SAR in the most recent ICNIRP guidelines for frequencies below 100 kHz [6].

A fair summary of the biological research results would be that they do not conclusively demonstrate evidence that proves or disproves a health risk from mobile-phone exposure. It is factual that more studies showed no health effect. However, except for the animal studies, a majority of the studies were short-term investigations. That includes epidemiological studies of head and neck cancers in mobile-phone users, as seen from previous articles in this column.

Nevertheless, the World Health Organization's International Agency for Research on Cancer (IARC) recently announced its conclusion, that while not entirely unanimous, acknowledged published scientific papers reporting increased risks for gliomas (a type of malignant brain cancer) and acoustic neuromas (a non-malignant tumor of the auditory nerve on the side of the brain) among heavy or

long-term users of cellular mobile telephones. Perhaps not surprisingly, some other groups of epidemiologists, reviewing the same data and papers, concluded that the increased risk was entirely explicable by various biases or errors. In their judgment, there was little possibility that mobile-phone use could increase the risk of glioma or acoustic neuroma in users.

References

1. CTIA, "News Release in Response to the Government Accountability Office (GAO) Report on Cell Phone Safety," CTIA-The Wireless Association, Washington DC, August 7, 2012.
2. GAO, "Exposure and Testing Requirements for Mobile Phones Should Be Reassessed," Government Accountability Office, Washington DC, August 7, 2012.
3. EWG, "GAO Tells FCC to Update Cell Phone Radiation Rules," The Environmental Working Group (EWG), August 7, 2012, http://www.ewg.org/release/gao-tells-fcc-update-cell-phone-radiation-rules.
4. J. C. Lin, "A New IEEE Standard for Safety Levels with Respect to Human Exposure to Radio Frequency Radiation," *IEEE Antennas and Propagation Magazine*, **48**, 1, February 2006, pp. 157-159.
5. ICNIRP, "Guidelines for Limiting Exposure to Time-Varying Electric, Magnetic, and Electromagnetic Fields (Up to 300 GHz)," *Health Physics*, **74**, 4,1998, pp. 494-522.
6. ICNIRP, "Guidelines for Limiting Exposure to Time-Varying Electric and Magnetic Fields (1 Hz – 100 kHz)," *Health Physics*, **99**, 6, 2010, pp. 818-836.

Wireless Battery-Charging Technology or Energy Harvesting to Power Mobile Phones or Other Mobile Communication Devices, and Health Effects

Wireless access to telephony or to the Internet via a smart phone or laptop computer is such a common-place everyday experience that it is hard for some folks to imagine that a connection to a pair of wires was the only way to make a telephone call in the not too distant past. Of course, routine wireless access also requires the nightly ritual of plugging in the smart phone or laptop via a power cable to an electrical outlet for it to be recharged, or more precisely, for the battery inside the mobile device to be recharged.

To most, battery charging through wireless power transfer is a novel approach, a potential niche technology for mobile applications. Indeed, for some proponents, before long, most people will be using wireless battery-charging technology or wireless energy harvesting to power cell phones or other mobile communication devices and for Internet access.

Without a doubt, recent interest and current optimism regarding battery-charging wireless power-transfer technology are driven by the ubiquity of cell phones and other mobile communication devices. The motivation isn't hard to find: a palpable, relentless drive toward ready access to the internet, information, or entertainment at any time in any place. In some ways this is to make a dream come true: a truly wireless mobile or portable communication device, completely free from being tethered in any way.

However, the concept of wireless power transfer, even for charging batteries, is not new. A case in point is harvesting energy from visible-light sources including the sun using solar cells, for powering a myriad of portable electronic devices and gadgets.

Obviously, each type of wireless power transfer has its unique characteristics and applications. Moreover, practical implementation of wireless power transfer in the form of transcutaneous power delivery for a wide variety of implanted medical devices has been around for quite some time, as well.

In medical applications such as the cardiac pacemaker – where the power requirement for operation is low – an implanted coil receives current from an external coil placed on the skin near the implanted coil. The typical separations between the internal and external coils are in the range of 1 cm to 2 cm. Through transcutaneous electromagnetic induction between the coils, the implanted coil directly provides the charging current for the pacemaker battery [1]. The typical frequency used to drive the coils is in the 10 kHz to 100 kHz range. However, the wireless power-delivery efficiency depends on the alignment between the external and the implanted coils. In other words, the coupling between the external and implanted coils will vary according to their orientation and other variable conditions, such as postural change. For implanted medical devices requiring moderate to high powers, resonant schemes have been applied to improve the coupling of the external and implanted coils.

On an almost opposite dimension, a grand vision of wireless power transfer employing space solar-power satellite (SPS-WPT) was conceived in the late 1960s [2].

James C. Lin is with the University of Illinois at Chicago, 851 S Morgan Street, M/C 154, Chicago, IL 60607-7053, USA; E-mail: lin@uic.edu.

(A version of this appeared in *IEEE Antennas and Propagation Magazine*, **55**, 2, April 2013; copyright 2013 IEEE.)

The concept of SPS-WPT envisions the generation of electric power by solar energy in space for use on Earth. The system would consist of an orbiting platform to gather solar energy and convert it to microwave power in space. A wireless (microwave) transmission system would be employed to send the power to Earth. A power-receiving antenna on the ground or Earth's surface would collect and convert the transmitted microwave energy into a form of electricity suitable for the common electric-utility distribution infrastructure.

Indeed, most of the concepts essential for SPS-WPT operation were successfully demonstrated in 1975 in an experiment conducted at Goldstone, California, among others. The Goldstone test was accomplished at a frequency of 2.45 GHz. Microwaves were beamed from a high-power dish antenna over a distance of 1.6 km to a receiving antenna. The point-to-point wireless power transfer demonstration produced 30 kW of dc power output at 84% efficiency [3]. The 2.45 GHz frequency is within the industrial, scientific, and medical (ISM) application band.

SPS-WPT is being viewed as an increasingly viable future energy source for competing with other sustainable energy candidates to meet the goal of providing sustainable energy for future growth and protection of the environment. The finite supply and parochial nature of energy resources, along with environmental concerns including waste management, are arguing more forcefully for SPS-WPT as a potential energy source to compete with other sustainable energy candidates.

It is interesting to note that a terrestrial, point-to-point wireless power transfer system was demonstrated on the French island of La Réunion, near Madagascar in the small mountain village of Grand-Bassin [4]. The village was surrounded by high canyon walls on all sides and had no electrical power supply, although it was close to a 4 kV transmission line located above the canyon. The 2.45 GHz wireless power transfer system was reported to have an overall efficiency of 50-70% for power transmission over a distance of 700 m across the canyon.

Today's mobile phones, tablets, and notebooks certainly still leave a lot to be desired from the perspectives of a power supply and convenience (a dead battery), and to some extent, from a safety point of view (having to use cables to plug in to an electrical outlet). Clearly, the first shortfall is because of the current limitations with the charged storage-battery technology not being able to provide a longer battery life. However, the second shortfall may be because of safety concerns (tripping over cables or being "zapped" by broken cables), or because cellular service users and customers are annoyed by or don't want to be bothered with having to plug the mobile device into an electrical outlet. If the latter is the case, as it appears to be, then time may well provide a fix to the grief. Indeed, the fix may happen much sooner than later.

As of this writing, several of the mobile-phone manufacturers and consumer electronics companies are advertising the latest wireless chargers, confident that wireless charging is the trend for future battery charging. For devices such as mobile phones, tablets, or notebooks, the wireless charging takes place locally, through electromagnetic induction between two separate coils respectively built inside the charger and the mobile device. Although they are electrically insulted from each other and are in separate enclosures, the two coils must be located very close to (in the near field of) each other, so that the electromagnetic coupling is sufficiently tight to achieve high charging efficiency. The magnetic field (typically in the kHz range) produced by the electric current flowing in the charging (transmitting) coil induces within the receiving coil an electric current used to charge the battery inside the mobile phone, for example. This is the simplest form of wireless power transfer, and is based on the same principle used for implanted medical devices. Electric shaver and toothbrush battery chargers also use this method.

Why the sudden interest in battery charging through wireless power transfer? Where is the novelty? Aside from not having to plug in the mobile phone or laptop, a more probable attraction derives from the potential for mobile communication devices to get their electrical power the same way they get their data: through the air, in locations within the field of reach of a wireless power transfer system. (In a way, this is like the connectivity afforded by Bluetooth: the capability to participate in an ad hoc network anytime two or more Bluetooth-enabled devices get within about 30 m of each other.)

This scheme of mobile communication devices receiving their electrical power through the air via inductive coupling is not new in itself: Nikola Tesla first proposed similar types of wireless power transfer years ago [5]. The resurgence of interest in inductive wireless power transfer schemes lies in the prospect that if massively deployed, they could open the door to transferring sufficient amounts of electrical energy to efficiently power mobile electronic devices without having to locate where the electrical power outlet is in relation to the mobile device.

In particular, a paper was presented by a group from the Massachusetts Institute of Technology at the 2006 Industrial Physics Forum in San Francisco. In it, they suggested the use of near-field electromagnetic inductive coupling for low-power applications, such as the charging of mobile phones and laptops [6]. There has been substantive interest in exploiting the concept. At least a couple of papers from the group have appeared in scientific journals since then [7-9].

The approach has been variously termed evanescent wireless power transfer, non-radiative power transfer, or weakly-radiative wireless energy transfer over a middle range, with a few meters between the power transmitter and the receiving device. More recently, some mention has

been made about operating ranges on the order of the size of a typical home, factory floor, or, perhaps, airport waiting lounges, for potential commercial applications.

There should not be any question about whether such a wireless power transfer system would work in concept, in the laboratory, or at close range. The key issues are power-transfer efficiency, the transmitted power requirements, and health and safety.

As described, the system would work in the near field of a lower-frequency electromagnetic source, at a distance of a few meters from the source. The propagation of electromagnetic energy into a region or a material medium at all frequencies can be divided into two principal zones from the source: the near field and the far field. The application in wireless communication mostly takes place in the far field, where the electric and magnetic fields form outgoing waves have plane wavefronts.

The near field consists of two components: the inductive component and the radiative component. The inductive component extends up to a distance of approximately one-sixth of a wavelength from the source, where the inductive and radiative components are equal to each other. For the inductive component, energy is stored in the electric and magnetic field during one-quarter of a cycle, and is returned to the source during the next one-quarter of a cycle, without a net or average outward flow. The power density associated with the inductive component is not as uniquely defined, and it varies from point to point. Its transverse distribution actually depends on the distance from the source, since the electric and magnetic fields and their ratios vary from point to point.

Electromagnetic power (even for sources that are predominantly magnetic in nature) is radiated. Its strength decreases with distance from the source as power flows away from the source via the radiative component. A large portion of this ultimately ends up as an average outward flow of electromagnetic power into the surrounding environment and beyond.

It is significant to note that the inductive component does not stop dead at a distance of one-sixth of a wavelength from the source. The electromagnetic energy radiated into the surrounding environment would be absorbed by objects, including humans and other biological organisms, in addition to the desired wireless power transfer for charging mobile phones and laptops.

If resonant inductive coupling is used, the transmitting and receiving coils may be designed for optimal wireless power transfer (and extraction of power from the transmitting source). Moreover, the spatial performance or useful range for wireless power transfer also may be improved by the increased coupling efficiency. However, in the process, the surplus electromagnetic power not transferred to a mobile device will remain in the immediate surrounding space to interact with other objects, including people, even if the objects resonate only weakly with the electromagnetic power.

Unlike wireless communication uses, the level of transmitted electromagnetic power required for large-scale or commercial implementation of wireless power transfer could be substantial. As part of the system design, serious attention should be given to preventing bodily harm from this (likely, high-source-power) application itself, let alone from the superposition of a new and strong source of electromagnetic field onto the existing ambient level in its domain of application. It is recommended that more emphasis be devoted to environmental, health, and safety efforts in order to assess the environmental, health, and safety impacts of the design, and to identify needed research if the impacts are not fully understood, early in the program.

(It is noted that a key feature of the SPS-WPT system design and research effort has been the consideration of biological effects and human safety. To assure environmental health and safety, the program has limited the "center-of-beam" power densities to the range of 100 W/m^2 to 200 W/m^2 (10 mW/cm^2 to 20 mW/cm^2) for wireless power transmission. The microwave power density was projected to be 1.0 W/m^2 (0.1 mW/cm^2) at the perimeter of the receiving antenna [10].)

References

1. A. W. Silver, G. Root, F. X. Byron, and H. Sandberg, "Externally Rechargeable Cardiac Pacemaker," *Annals of Thoracic Surgery*, **1**, 1965, pp. 380-388.
2. P. F. Glaser, "Power from the Sun: Its future," *Science*, **162**, 1968, pp. 857-866.
3. W. C. Brown, "The History of Power Transmission by Radio Waves," *IEEE Transactions on Microwave Theory and Techniques*, **32**, 1984, pp. 1230-1242.
4. J. D. Lan Sun Luk, A. Celeste, P. Romanacce, L. Chane Kuang Sang, and J. C. Gatina, "Point-to-Point Wireless Power Transportation in Reunion Island," 48th International Astronautical Congress, Turin, Italy, October 1997 (also available at http://www.science-sainte-rose.net/GrandBassin/ wpt01/ sessions.htm).
5. N. Tesla, *Experiments with Alternating Currents of High Potential and High Frequency*, New York, McGraw-Hill, 1905.
6. M. Soljacic, A. Karalis, and J. D. Joannopoulos, American Institute of Physics Industrial Physics Forum, San Francisco, November 2006.
7. A. Kurs, A. Karalis, R. Moffat, J. D. Joannopoulos, P. Fisher, and M. Soljačić, "Wireless Power Transfer via Strongly Coupled Magnetic Resonances," *Science*, **317**, 2007, pp. 83-86.
8. R. E. Hamam, A. Karalis, J. D. Joannopoulos, and M. Soljačić, "Efficient Weakly-Radiative Wireless Energy Transfer: An EIT-Like Approach," *Annals of Physics*, **324**, 2009, pp. 1783-1795.
9. A. Kurs, R. Moffatt, and M. Soljačić, "Simultaneous Mid-Range Power Transfer to Multiple Devices," *Applied Physics Letters*, **96**, 2010, p. 102.
10. J. C. Lin, "Space Solar-Power Station, Wireless Power Transmission, and Biological Implications," *IEEE Antennas and Propagation Magazine*, **43**, 3, June 2001, pp. 166-169.

Scattering Analysis of Periodic Structures Using Finite-Difference Time-Domain Method

by Khaled El Mahgoub, Fan Yang, and Atef Elsherbeni, San Rafael, CA, Morgan & Claypool Publishers, May 2012, 140 pp. DOI:10.2200/S00415ED1V01Y201204CEM028), series ISSN: 1932-1252 (print) 1932-1716 (electronic),

The scope of the book is an up-to-date, efficient, numerical approach for the electromagnetic-field simulation of periodic structures using the FDTD technique. The development of these structures has gained increasing importance in the course of the past few years. This is due to a number of emerging engineering applications, such as frequency-selective surfaces, bandgap structures, antenna arrays, metamaterials, and many others. Correspondingly, major efforts have been made by several researchers to develop appropriate numerical methods for the analysis of these structures.

The book focuses on a specialized FDTD technique, implementing periodic boundary conditions by means of the constant-wavenumber method. This particular time-domain method was developed by the authors themselves, and it was presented earlier in a series of technical articles in scientific journals. The book provides a comprehensive survey of these developments, including a large number of practical examples, as well as extensive implementation details. Written by experts in the field, the book is a must for graduate students and engineers who intend to apply this approach in the numerical modeling of periodic structures.

The book consists of six chapters and two appendices covering the most important cases encountered in the modeling of periodic structures. The reader is conducted step-by-step into the modeling aspects of this class of problems. This is done by starting with the basic formulation of the constant-wavenumber method, and then introducing increasingly more complicated simulation models, such as dispersive and multilayer periodic structures.

After giving a brief introduction of the topic in Chapter 1, the authors start in Chapter 2 with an introduction to the classical FDTD method. This is done in great detail by providing the full set of update equations for all field components. Although the resulting lengthy equations could be somewhat confusing for the inexperienced reader, they offer a good basis for those researchers and engineers intending to themselves implement a simple variant of the FDTD technique for their own applications. In this chapter the authors also introduce the periodic boundary conditions based on the constant-wavenumber approximation. The numerical necessity for the application of this approach is nicely motivated. However, the reader may find it difficult to develop an in-depth understanding of the physical meaning of the approximation used at this stage. What is the interpretation of the complex fields in the time domain is thus not immediately apparent. The causality issues related to this approximation, their origin, and their numerical implications are also very swiftly mentioned, in no more than a single sentence in the whole book. The reader is at times confronted with important terms and issues (such as the problem of horizontal resonances) that are not further explained and are thus difficult to follow without further consulting specialized literature. These deficiencies are partially compensated for by the detailed description of code implementation, and by the application examples presented in the second part of the chapter.

In Chapter 3, the authors provide the necessary technical modifications of the method when skewed-grid periodic structures are considered. Two cases are discussed: the coincident and the non-coincident grid-skewed shift. The accuracy of this approach is demonstrated in a number of simulation examples, including various types of frequency-selective surfaces. Again, an in-depth analysis of the method (supporting, e.g., the statement on the numerical stability in the non-coincident grid case) is partially missing, although this could have been useful for readers interested in the numerical properties of the method.

In Chapter 4, the method is further developed for the more-complicated case of dispersive periodic structures. The authors first describe the auxiliary differential equation method as commonly used in the FDTD simulation of Debye and Lorentz media. They then combine this approach with the constant-horizontal-wavenumber method for periodic structures. A thorough description of the single implementation steps is provided, including the case where periodic boundaries are located within dispersive materials. A number of simulation examples is given, including the important application case of a nano-plasmonic solar-cell structure. For each of the presented examples, the authors provide validation studies where the FDTD technique with periodic boundaries is compared with numerical results obtained with conventional frequency-domain methods, using the commercial codes Ansoft *Designer* and *HFSS*.

The more-general case of multilayered structures is discussed in Chapter 5. The authors introduce important concepts, such as Floquet-mode analysis and the Generalized Scattering Matrix formalism. These are of interest not

only in the modeling of periodic structures, but also in the more-general context of electromagnetic-field computation. Furthermore, the authors discuss the implementation of periodic boundary conditions with the constant-horizontal-wavenumber approach, as well as deriving conditions for selecting the proper gap size to reduce the number of harmonics needed in the Floquet modal analysis.

Summarizing, this is overall a good book, even though the reader may occasionally miss the kind of in-depth analysis that makes "numerics" trustworthy. However, the main strength of the book consists of the extensive technical description of algorithms, their implementation, and the simulation examples. As such, it is in particular worthwhile for graduate students and engineers interested in the implementation of a numerical code for the simulation of periodic structures.

Reviewed by:

Erion Gjonaj
Computational Electromagnetics Laboratory (TEMF)
Technische Universität Darmstadt
Schlossgartenstr. 8, 64289 Darmstadt, Germany
E-mail: gjonaj@temf.tu-darmstadt.de

[Editor's note: The Young Scientists who received an award at the 2011 Istanbul URSI GASS were asked to review their favorite textbook, even if it was a classic book. This is in contrast to our usual reviews, where we try to have new books reviewed. The review below is from a Young Scientist.]

Fundamentals of the Physical Theory of Diffraction

by Pyotr Ya. Ufimtsev, New York, Wiley/IEEE Press, 2007, 329 pp., ISBN: 9780470097717.

Diffraction is one of the most popular fields of scattering problems. Exact solutions of scattering problems that satisfy the boundary conditions can be obtained by solving Helmholtz's wave equation. In order to solve Helmholtz's wave equation, the separation-of-variables technique is used for suitable scattering geometries. In some cases, the separation-of-variables technique is not applicable, especially for complex geometries. For these kinds of situations, high-frequency asymptotic techniques are preferred. High-frequency asymptotic techniques can be divided into two groups. The first group consists of the ray-based techniques, and the second group consists of the integral-based techniques. The Physical Theory of Diffraction (PTD) is one of the well-known integral-based techniques. This technique has proven its efficiency not only in science, but also in the field of technology. To illustrate, the PTD has played a key role in the development of modern low-radar-reflectivity weapons. This book presents the fundamental concepts of the method for both acoustic and electromagnetic-wave diffraction. It is a most fundamental book for researchers and graduate students who are especially interested in the diffraction process.

This book consists of fourteen chapters. It can be divided into three main parts. In the first part, the author tries to explain the concepts on which the PTD is based. In the second part, he obtains the nonuniform part. The last part is allocated to various applications.

Chapter 1 includes the formulation of the diffraction problems, the description of the scattered fields in the far zone, basic definitions of Physical Optics (PO) concepts, and the nonuniform components of the induced surface field and electromagnetic waves. In this chapter, the author focuses on the explanation of the PO approximation. Physical Optics is also a high0frequency asymptotic technique, which is used for investigation of the scattered fields from large metallic objects.

Chapters 2, 3, and 4 are related to each other. The mutual concept is investigation of wedge diffraction. In Chapter 2, the author gives a detailed explanation of the solution of wedge diffraction, because the wedge-diffraction problem is the basis for the construction of the PTD. The author first obtains the infinite-series solution of the wedge problem. He then converts it into the Sommerfeld integral expression, which is convenient for asymptotic analysis. He lastly derives the uniform asymptotic expressions for the wedges. In Chapter 3, the PO part of the scattered field is calculated. The PO field results from the induced source's uniform component. Later on, this calculated uniform part is used for an examination of the nonuniform source as the difference between the exact and PO fields. In Chapter 4, integral and asymptotic representations of the nonuniform components of the surface sources are constructed as a result of the previous sections. From this point on, the contribution of the nonuniform component is investigated.

In Chapter 5, the PTD method that has been built in the previous chapters is applied to strips and cylinders with triangular cross sections. The contributions of the uniform and nonuniform components of the surface sources to the scattered field are investigated. The solutions are also numerically investigated.

In Chapter 6, the author develops the first-order PTD for acoustic waves scattered from sharp edges. The diffraction of waves from conic surfaces, cones, disks, and curved surfaces is investigated in terms of uniform and nonuniform components.

In the previous chapters, the contributions of the edge-diffracted waves to the scattered fields were investigated. In Chapter 7, the aim is to derive the high-frequency asymptotics for elementary edge waves (EEWs). The edge-diffracted waves are represented by the superposition of the elementary edge waves, where the elementary edge waves are the waves that are created by the induced fields over the infinitesimal length of the edges.

In Chapter 8, the author makes a comparison between ray asymptotics and the PTD. He proposes that in terms of the total scatting field, the Geometrical Theory of Diffraction (GTD) can be interpreted as the ray-asymptotic form of the PTD. He mentions that the GTD is not applicable in regions where the field does not have a ray structure. He establishes a similarity between the electromagnetic and acoustic waves.

In Chapter 9, two important situations for diffraction are investigated according to the acoustic and electromagnetic waves. The first situation is grazing incidence, which can be described as the incident waves propagating parallel to the plates. The second case is slope diffraction. This case occurs when the scattering edge is located in a zero of the incident waves.

In Chapter 10, the author investigates the diffraction interaction of two edges for acoustically hard and soft surfaces, and also for electromagnetic waves.

In Chapters 11 and 12, the author focuses on multiple-edge diffraction for different problems. In Chapter 11, multiple diffractions of waves over a flat base are investigated for the situations where both the source and the observation points are on-axis. In Chapter 12, the disk diffraction problem is again discussed, but this time where edge waves propagate on both faces of the disk.

In Chapter 13, backscattering from a finite-length cylinder that is illuminated by a plane wave is investigated. The contribution of the nonuniform component is analyzed, and the numerical results in terms of PO and the PTD are given.

In Chapter 14, the scattered fields from a flat cylinder are investigated in terms of acoustic and electromagnetic waves. The PTD analysis of a rigid cylinder is investigated.

In general, this book is based on Ufimtsev's research as reported in the literature. The fundamental concepts of the PTD are introduced into this book. The PTD allows the calculation of the contribution of nonuniform components to the scattered fields. It is an important point for investigation of antenna radiation characteristics and scattering. It is an important method in the study of complex problems of diffraction. As mentioned before, this book is one of the fundamental sources treating diffraction for researchers and graduate students.

Reviewed by

Husnu Deniz Baasdemir
Cankaya University
Department of Electronic and Communication Engineering
Ankara, Turkey
E-mail: basdemir@cankaya.edu.tr

Conferences

CONFERENCE REPORTS

5th VLF/ELF Remote Sensing of Ionosphere and Magnetosphere (VERSIM) Workshop

São Paulo, Brazil, 3 - 6 September 2012

The working group on VLF/ELF Remote Sensing of the Ionosphere and Magnetosphere (VERSIM) is an international group of scientists interested in studying the behavior of the magnetosphere and ionosphere by means of ELF (300 Hz to 3 kHz) and VLF (3 kHz to 30 kHz) radio waves, both naturally and artificially generated. The group was set up in 1975 by URSI and IAGA. At present, the main subjects of interest include plasma structures and boundaries: morphology and dynamics, wave-particle and wave-wave interactions, wave-induced particle precipitation, wave propagation in the magnetosphere and ionosphere, sprites, and the effects of lightning on the ionosphere.

The VERSIM workshop is a biennial scientific meeting that brings together a community of scientists from 26 countries. The fifth VERSIM workshop was held at the Presbyterian Mackenzie University, São Paulo, Brazil, on September 3-6, 2012. Local institutional support came from the Center for Radioastronomy and Astrophysics Mackenzie (CRAAM), and the National Institute for Space Research (INPE). Financial support was provided by Fundo de Pesquisa Mackenzie, Fundação de Amparo à Pesquisa do Estado de São Paulo, ICSU, IAGA, and URSI (Commissions G and H). The meeting was intended to bring together experts in the areas of VLF/ELF research from well-known scientific institutions. A specific achievement of the workshop was a fruitful interaction between scientific professionals and regional students from Brazil, Peru, Ecuador and Uruguay.

The meeting was attended by 58 participants from the five continents, including researchers and students. This was the first VERSIM Workshop held outside Europe. 56 papers in the form of talks and posters were presented during scientific sessions focused on: (i) sub-ionospheric propagation, observations and modeling; (ii) VLF chorus emissions and quasi-periodic emissions; (iii) triggered emission and wave-particle interactions; (iv) induced emissions and diagnostic in optical and radio range; (v) VLF data sets and campaigns; (vi) a geophysical approach to assess natural disasters and space weather impacts on earth.

Among the scientific highlights of the meeting, Dr. C. Rodger showed results of the World Wide Lightning Location Network (WWLLN), Dr. P. Hansen presented information on the VLF transmitter systems maintained by the U.S. Navy, Dr. K. Lynn showed results concerning asymmetries in VLF propagation and their effects. Dr. M. Rycroft presented a talk about the South Atlantic geomagnetic anomaly and its link to the preferred meridian for electron-whistler interactions in the magnetosphere. Dr. S. Cummer discussed a technique based on measurements of broadband VLF radiation from lightning to investigate the variability of the ionospheric D region. Dr. J. Lichtenberger presented new results on automatic detection and analysis of whistlers (Automatic Whistler Detector and Analyzer, AWDA). Dr. D. Shklyar showed results of studies of propagation of ELF waves in the magnetosphere.

In a special session on devoted to geophysical tools, Dr. F. Lefeuvre (former President of URSI) gave a talk on the current URSI prevention programs and management of natural hazards. Dr. J.-P. Raulin presented results and prospects of the project "A Geophysical Approach to Assess Natural Disasters and Space Weather Impacts on Earth," which was supported by ICSU and URSI. Dr. C. Valladares presented recent results of the "Low Latitude Ionospheric Sensor Network (LISN)" of GPS sensors to calculate the total electron content (TEC) and ionospheric scintillations. Mr. R. Godinho, Departamento de Controle do Espaço Aéreo (DECEA, Department of Airspace Control) showed aspects of flight control through positioning systems for aviation. Finally, Dr. J. Costa, Instituto Nacional de Pesquisas Espaciais (INPE, National Institute for Space Research) presented the program of "Estudo e Monitoramento Brasileiro do Clima Espacial" (EMBRACE, center for studies and monitoring of space weather).

A VERSIM business meeting was organized at the end of the workshop by VERSIM co-Chairs Dr. J. Lichtenberger (URSI co-Chair) and Dr. C. Rodger (IAGA co-Chair). The participants of this business meeting acknowledged and approved the suggestion of Dr. C. Rodger to organize the next edition (sixth) of the VLF/ELF Remote Sensing of Ionosphere and Magnetosphere (VERSIM) Workshop at the University of Otago in Dunedin, New Zealand, on January 20-23, 2014.

Ondrej Santolik
E-mail: os@ufa.cas.cz
URSI representative at the 5th VERSIM workshop with input provided by C. Rodger, J.-P. Raulin, and F. Bertoni

International Symposium on Signals, Systems and Electronics (ISSSE'2012)

Potsdam, Germany, 3 - 5 October 2012

The ISSSE'2012 (International Symposium on Signals, Systems and Electronics) is held every three years, and is organized under the guidance and with sponsorship of the international steering committee of the URSI Commissions C (Radiocommunication Systems and Signal Processing) and D (Electronics and Photonics). Since antennas form an essential part of radio communication systems, aspects of URSI Commission B (Fields and Waves) are also usually included into the technical scope of the symposium.

The main topics of the conference include: Electronics for Communications, Sensing and control, Circuits & Systems Design and simulation, Coding, Channel, Modulation, Detection Strategies, SDR and Cognitive radio, Photonic techniques and systems, RF, Microwave and Wireless systems, Devices and techniques for RF, Microwave and photonics, Emerging materials and technologies, Numerical and CAD Techniques, Radio channels (relay and cooperative channels, vehicular channels, body area channels), and Networks & Signals. Application topics addressed in the conference were Radar, Smart Antennas/MIMO Techniques and RFID and NFC technologies and applications.

In 2012 the symposium was exceptionally held after two years in Potsdam, Germany and was organized by the Innovations for High Performance Microelectronics, IHP and the Heinrich Hertz Institute, Fraunhofer HHI. The conference was sponsored by Cadence and Rohde and Schwartz and various exhibitors of radio equipment such as the HHI high rate high performance digital radio testbed and the IHP mm wave and optical testbeds. In addition to URSI, Technical co-sponsors included the IEEE region 8, MTT-S, EuMA, the IET and COST IC1004. The social programme and the friendly atmosphere of the conference enabled the networking and scientific discussions.

The conference had three invited sessions, fifteen regular oral sessions and a poster session. Each of the three invited sessions was preceded by a key note speech delivered on each day of the Symposium. The first session chaired by Sana Salous addressed Green radio for smart environments with a key note speech delivered by Dr. Robert Bultitude from the Communications Research Centre, Ottawa Canada on Temporal and spatial variability on urban mobile radio channels and the potential for performance gains in systems using radio technology that can adapt to such variability. Four papers were delivered in the session on efficient and fair radio resource allocation for spontaneous multi-radio wireless mesh networks, indoor radio coverage solutions based on interleaved-MIMO DAS, cooperative wireless network coding for uplink transmission on hierarchical wireless networks, and a realistic reference simulation environment for typical urban areas.

The second session chaired by Ingmar Kallfass addressed applications of Terahertz Electronics: Prospects and Challenges. The keynote speech was delivered by Kei Sakaguchi from Tokyo Institute of Technology, Japan on Basestation cooperation (CoMP) is ready for standardization and deployment followed by three invited papers on weather robustnesss of THz communications exemplified with emulated dust, waveform diversity in Terahertz sensing applications, and transistor based integrated receivers for THz applications.

The third session chaired by Thomas Kaiser who also delivered the key note speech addressed cognitive radio - technology and applications. Three invited papers addressing RF frontends requirements for cognitive radio, multicarrier transmission schemes in cognitive radio, and success factors for spectrum sharing.

The conference covered microwave radio links and design of mm wave systems. An example is the paper that discusses the influence of climatic parameters namely the refractivity gradient (dN1), the geoclimatic factor (K), rain, temperature, pressure, and humidity on microwave telecommunications links. The impact of these parameters which increases with frequency is shown to highly alter the performance of terrestrial links. Based on data collected from terrestrial links located in Quebec (Canada) seasonal variation of the geoclimatic factor, Kmes is quantified and the variations are correlated with the variation of humidity. Since ITU recommendations assume a stationary climate and do not embed climate change, the paper recommends improving predictive models by taking into account the long-term temporal changes. Another paper reported on a wireless 60 GHz OFDM transceiver for a high throughput GigE Vision standard compliant colour CCD camera system used in machine vision applications. The work describes an OFDM transceiver which provides net data rates up to 3.9 Gb/s and a medium access controller (MAC) which offers the reliable GigE point-to-point cable replacement functionality with special support of an asymmetrical downlink scenario. The OFDM baseband processor (BB) and the MAC were fully implemented in FPGA technology.

Other papers addressed multiple antenna technology such as the paper that discusses the influence of the antenna configuration on the achievable throughput in a real indoor propagation environment for 2-by-2 single-user (SU) multiple-input multiple-output (MIMO) in the Long Term Evolution (LTE)-Advanced uplink using single carrier-based radio access. Indoor experiments conducted in an office at walking speed, with four antenna configurations: co-polarized antennas with a long or small separation, cross-polarized antenna, and a distributed antenna arrangement were used to evaluate rank-2 MIMO spatial

multiplexing. The results show that the cross-polarized antenna configuration achieves a higher user throughput than the other antenna configurations. In addition when closed-loop rank-1 precoding is applied, the cross-polarized antenna configuration is effective in stably achieving a relatively-high throughput regardless of the tilt angle of the mobile station transmitter antenna, although the other antenna configurations indicate better throughput under ideal antenna-tilt angle conditions. Another paper studies the effect of severe oscillator phase noise which gives rise to inter-carrier interference that becomes a limiting factor in sustaining a reliable communication link in an orthogonal frequency division multiplexing receiver in spatially multiplexed MIMO channels. It proposes an iterative algorithm employing low-complexity phase noise mitigation to alleviate degradation in the channel estimation and the data detection stages taking advantage of the approximate sparsity pattern inherent to the phase noise spectral composition and exploiting decoupled compensators. The proposed scheme enhances the receiver performance while retaining a modest complexity. Moreover, the simplified estimator efficacy is demonstrated when a generalized oscillator signal distribution network feeds the radio paths of the multiple receiver front-ends.

Other papers covered RF networks such as the paper which analyses the bit error rate performance and error vector magnitude of a tunable impedance matching network using QPSK, 16-QAM and 64-QAM digital modulation schemes. The characterized RF-network is based on Barium-Strontium-Titanate ferroelectric thick-lm varactors for tunable impedance matching. Inherent dispersive behaviour is subsumed in the forward transmission of the passive device. Due to this nonlinear phase response, in general to maximize the overall system performance, an agile selection of the varactor values is demonstrated, taking into account the phase and group delay of s21 parameter. Detailed signal simulation results based on measured data of a testbed are presented and the influence of varying matched impedances on the tuning behavior with different modulation bandwidths is discussed at a center frequency of 1.9 GHz.A number of other papers on FMCW radar were presented which included through wall imaging, synchronous signal detection and processing, including CMOS technology for processing radar signals in the 24 GHz band.

Prof. Sana Salous
sana.salous@durham.ac.uk
URSI representative at the ISSSE'2012 Meeting

CONFERENCE ANNOUNCEMENT

IRI Workshop

Olsztyn, Poland, 24 - 28 June 2013

The 2013 International Reference Ionosphere (IRI) Workshop will be held at the University of Warmia and Mazury (UWM) in Olsztyn, Poland from June 24 to 28, 2013. The workshop will be hosted by the Department of Astronomy and Geodynamics of UWM with Andrzej Krankowski as the Local Organizer. IRI is a joint project of the Committee on Space Research (COSPAR) and the International Union of Radio Science (URSI) that brings together ionospheric modelers and experimenters with the goal of developing and improving a data-based international reference model for the ionosphere.

Olsztyn is a 3-hour bus ride from the Warsaw International Airport (Chopin). Transfer between the airport and Olsztyn hotels will be organized.

Topics

The focus of this year's workshop will be on "IRI and GNSS". Key topics covered will include:

- Improvements of IRI with Global Navigation Satellite System (GNSS) data
- GNSS monitoring of ionosphere (TEC, fluctuation and scintillation effects)
- Real-Time IRI including the representation of storm-time effects
- Modeling the high latitudes ionosphere
- Mapping of ionospheric peak parameters
- The Ionosphere and IRI during the recent solar cycle
- New inputs for IRI
- IRI Applications

Submission Deadline

The conference website is at http://www.uwm.edu.pl/kaig/iri_workshop_2013.

The deadline for submission of abstracts is March 15, 2013.

Contact

IRI homepage : http://iri.gsfc.nasa.gov.
Dieter Bilitza : dbilitza@gmu.edu
Andrzej Krankowski : kand@uwm.edu.pl

URSI CONFERENCE CALENDAR

April 2013

EUCAP 2013 - The Seventh European Conference on Antennas and Propagation
Gothenburg, Sweden, 8-12 April 2013
Contact: Eucap2013@realize-events.de, Jennifer at +49-89-660799-420 and registration@eucap2013.org
http://www.eucap2013.org/

URSI Benelux Forum 2013 - New Application Domains of Radio Science
Eindhoven, the Netherlands, 19 April 2013
Contact: Mark Bentum, E-mail: M.J.Bentum@utwente.nl, http://www.ursi-nederland.nl/index.htm

URSI-F-TS - URSI Commission F Triennial Open Symposium on Radiowave Propagation and Remote Sensing
Ottawa, ON, Canada, 30 April - 3 May 2013
Contact: Radio Propagation: Dr R.J. Bultitude, Communications Research Centre, Satellite Comm. & Radio Propagation, 3701 Carling Avenue, Ottawa, ON K2H-8S2, Canada, E-mail : robert_bultitude@ursi-f-ts.com
Remote Sensing: Brian_Brisco@ursi-f-ts.com

May 2013

EMTS 2013 - URSI Commission B International Symposium on Electromagnetic Theory
Hiroshima, Japan, 20-23 May 2013
Contact : Prof. G. Manara, Dept. of Information Engineering, University of Pisa, Italy, E-mail g.manara@iet.unipi.it, Website : http://ursi-emts2013.org

June 2013

RAST 2013 - New ways of Accessing Space for the Benefit of Society
Istanbul, Turkey, 12-14 June 2013
Contact : RAST2013 Secretariat, Turkish Air Force Academy (Hava Harp Okulu), Yesilyurt, Istanbul, Turkey, Fax : +90 212 6628551, E-mail : rast2013@rast.org.tr, http://www.rast.org.tr

MSMW '13 - 8th International Kharkov Symposium on Physics and Engineering of Microwaves, Millimeter and SubMillimeter Waves
Kharkiv, Ukraine,23 -28 June 2013
Contact: Dr. A. Linkova, Institute of Radiophysics and Electronics, National Academy of Sciences of Ukraine, 12 Acad. Proskura Street, Kharkiv - 61085, Ukraine, fax: +38 057 315-21-05, e-mail: gannalinkova@gmail.com, http://www.ire.kharkov.ua/MSMW13/Session.htm

IRI Workshop 2013 - International Reference Ionosphere (IRI) Workshop 2013 - IRI and GNSS
Olsztyn, Poland, 24-28 June 2013
Contact: iri2013@uwm.edu.pl, http://www.uwm.edu.pl/kaig/iri_workshop_2013/

July 2013

IconSpace 2013 - 2013 International Conference on Space and Communication
Malacca, Malaysia, 1-3 July 2013
Contact: iconspace@ukm.my
http://www.ukm.my/iconspace2011/

Beacon Satellite Meeting
Bath, Uk, 8-12 July 2013
Contact: Ms. Patrica Doherty, Boston University School of Management, 595 Commonwealth Avenue, Boston, MA 02215, USA, E-mail : pdoherty@bu.edu, Website : http://www.bc.edu/research/isr/ibss.html

August 2013

HF 13 - The Tenth Nordic HF Conference HF 13 with Longwave Symposium LW 13
Faro, Sweden (Baltic Sea), 12-14 August 2013
Contact: Carl-Henrik Walde, HF 13 chair, info@walde.se
http://www.nordichf.org/index.htm?index2.htm&2

ISRSSP 2013 - Third International Symposium on Radio Systems and Space Plasma
Sofia, Bulgaria, 28-30 August 2013
Contact: IICREST c/o B. Shishkov (ICTRS 2013 Event); P.O. Box 104; 1618 Sofia; Bulgaria, E-mail: bshishkov@math.bas.bg
http://www.isrssp.org/

September 2013

EMC Europe 2013 Brugge
Brugge, Belgium, 02-06 September 2013
Contact: Davy Pissoort, Head FMEC, Zeedijk 101, B8400 Oostende, Belgium, Fax: +32 59 56 90 01, E-mail: davy.pissoort@khbo.be, http://www.emceurope2013.eu

AP-RASC 2013 - AsiaPacific Radio Science Conference
Tapei, China SRS, 3-7 September 2013
Contact : Prof. K. Kobayashi, Chair, AP-RASC International Advisory Board, Fax: +886 2 23632090, E-mail: ctshih@tl.ntu.edu.tw, Website : http://aprasc13.ntu.tw

AFRICON 2013 - Sustainable Engineering for a Better Future
Mauritius, 9-12 September 2013
Contact: generalchair@africon2013.org, http://africon2013.org/

ICEAA-APWC-EMS conferences
Torino, Italy, 9-13 September 2013
Contacts: Prof. W.A. Davis, EMS Chair wadavis@vt.edu and Prof. Y. Koyama, EMS Vice-Chair koyama@nict.go.jp, http://www.iceaa.net

Metamaterials 2013 - The Seventh International Congress on Advanced Electromagnetic Materials in Microwaves and Optics
Bordeaux, France, 16-21 September 2013
Contact: Prof. Sergei A. Tretyakov, Dept. Of Radio Science and Engineering, Aalto, School of Electrical Engineering, PO Box 13000, FI-00076 Aalto, Finland, E-mail: sergei.tretyako@aalto.fi, fax: +358 9 470 22152, http://congress2013.metamorphose-vi.org/

October 2013

Microwave Signatures 2013 - Specialist Symposium on Microwave Remote Sensing of the Earth, Oceans, and Atmosphere
Espoo (Helsinki), Finland, 28-31 October 2013
Contact: Prof. Martti Hallikainen, Aalto University, School of Electrical Engineering, Department of Radio Science and Engineering, E-mail: info.frs2013@ursi.fi
http://frs2013.ursi.fi/

November 2013

First COSPAR Symposium - Planetary Systems of our Sun and other Stars, and the Future of Space Astronomy
Bangkok, Thailand, 11-15 November 2013
Contact: E-mail:cospar2013@gistda.or.th, http://www.cospar2013.gistda.or.th/

December 2013

ICMAP 2013 - International Conference on Microwaves and Photonics
Dhanbad, India, 13-15 December 2013
Contact: http://icmap2013.org/

January 2014

VERSIM-6 - Sixth VERSIM Workshop
Dunedin, New Zealand, 20-23 January 2014
Contact: Prof Craig J. Rodger, Department of Physics, University of Otago, PO Box 56, Dunedin 9016, NEW ZEALAND, Fax: +64 3 479 0964, E-mail: crodger@physics.otago.ac.nz

April 2014

RADIO 2014 - Radio and Antenna Days of the Indian Ocean 2014
Flic-en-Flac, Mauritius, 7-10 April 2014
Contact: Conference Secretariat RADIO 2012, University of Mauritius, Réduit, Mauritius, Fax: +230 4656928, E-mail: radio@uom.ac.mu, http://sites.uom.ac.mu/radio2012/

August 2014

COSPAR 2014 ("COSMOS") - 40th Scientific Assembly of the Committee on Space Research (COSPAR) and Associated Events
Moscow, Russia, 2 - 10 August 2014
Contact: COSPAR Secretariat, c/o CNES, 2 place Maurice Quentin, 75039 Paris Cedex 01, France, Tel: +33 1 44 76 75 10, Fax: +33 1 44 76 74 37, cospar@cosparhq.cnes.fr
http://www.cospar-assembly.org/

September 2014

EMC Europe 2014
Gothenburg, Sweden, 1-4 September 2014
Contacts: Symposium Chair: jan.carlsson@sp.se, Technical Program Chair: peterst@foi.se
http://www.emceurope2014.org/

An up-to-date version of this conference calendar, with links to various conference web sites can be found at http://www.ursi.org/en/events.asp

URSI cannot be held responsible for any errors contained in this list of meetings

THE EIGHTH INTERNATIONAL KHARKOV SYMPOSIUM ON PHYSICS AND ENGINEERING OF MICROWAVES, MILLIMETER, AND SUBMILLIMETER WAVES (MSMW'13) AND WORKSHOP ON TERAHERTZ TECHNOLOGY (TERATECH'13)
Kharkiv, Ukraine, June 23-28, 2013

ANNOUNCEMENT • MSMW'13 & TERATECH'13 • CALL FOR PAPERS

Organized by: The Scientific Council of the National Academy of Sciences of Ukraine on Radio Physics and Microwave Electronics in collaboration with IRE NASU, IRA NASU, IMag NASU and MESU, KhNU, KhNURE **with the support of the following organizations:** IEEE AP/MTT/ED/AES/GRS/NPS/EMB Societies East Ukraine Joint Chapter, IEEE MTT/ED/AP/CPMT/SSC Societies West Ukraine Joint Chapter, IEEE MTT/ED/COM/CPMT/SSC Societies Central Ukraine Joint Chapter, Ukrainian National URSI Committee. The support of the IEEE AP, MTT, ED, NPS, and AES Societies and URSI is under negotiation

Introduction: The Eighth International Kharkov Symposium on Physics and Engineering of Microwaves, Millimeter and Submillimeter Waves (MSMW'13) will be held in Kharkov, Ukraine, on June 23-28, 2013. The Workshop on Terahertz Technology (TeraTech'13) will be organized within the symposium. During the symposium, a one-day workshop "Complex Conductivity and Wave Symmetry of Fe-Based Superconductors" is also planned**.** These events will be sponsored by the National Academy of Sciences of Ukraine (NASU) Scientific Council on Radio-Physics and Microwave Electronics and A. Usikov Institute for Radiophysics and Electronics of NASU. IRE NASU has always been one of the major Ukrainian research organizations in this field. It was established in 1955 with the main tasks of developing the mm-wave vacuum sources, wave propagation and radars, and hot-plasma diagnostic systems for Tokamak controlled fusion machines; later it was involved in the development of in-orbit remote sensing and communication systems. The main collaborating organizations are the Institute of Radio Astronomy (IRA) of NASU, which branched off IRE in 1985 and leads research in the mm-wave radars and radio astronomy; Institute of Magnetism (IMag) of NASU; Ministry of Education and Science of Ukraine (MESU), which was founded in 1995 and performs research into modern problems of the physics of magnetism and magnetic materials; V. Karazin Kharkov National University (KhNU), the third oldest (since 1804) and highly reputed university in natural sciences in the former Soviet Union (FSU); Kharkov National University of Radio Electronics (KhNURE), a technical university in Ukraine entirely in electronics and computers; three Ukrainian IEEE Joint Chapters; and the Ukrainian National URSI Committee. MSMW symposia were held several times in Kharkov since 1978 as regular FSU meetings on mm and sub-mm waves and applications. It became a major event in this area and since 1991 it has been known as the International Kharkov Symposium - MSMW.

Transportation Connections: Every day Kharkov is accessible by direct flights of the Austrian Airlines from Vienna and Pegasus Airlines from Istanbul. International air connections are available to Kiev with numerous daily flights. This is to be followed by a one-hour flight or an overnight train to Kharkov, 450 km to the east. It is also possible to reach Kharkov via Moscow, but in this case a Russian double-transit visa should be obtained. Every possible assistance will be provided as long as any problems may arise.

Visa: No visa is required for the citizens of the EU, Israel, Norway, Switzerland, Turkey, the USA, Canada, and Japan. The participants from the other countries need a valid visa to enter Ukraine. The Organizing Committee will send official invitation letters to the authors of all accepted papers.

Young Scientist Travel Grants: Travel grants might be expected to help young scientists from FSU and developing countries to attend the MSMW'13 & TERATECH'13. The number and amount of grants will depend on the success of the on-going search for sponsors.

Suggested Sessions

W. Workshop on Terahertz Technologies
I. Electromagnetic theory and numerical simulation
II. Waves in semiconductors and solid state structures
III. Microwave superconductivity
IV. Wave propagation, radar, remote sensing and signal processing
V. Vacuum electronics
VI. Solid state devices
VII. Antennas, waveguide and integrated circuits
VIII. Radio astronomy and Earth's environment study
IX. Radiospectroscopy, complex media, nanophysics
X. Scientific, industrial and biomedical applications
XI. R-functions, atomic functions, wavelets, fractals

MSMW'13 Chair: Prof. Vladimir M. Yakovenko (IRE NASU). **MSMW'13 Co-Chairs:** Prof. Leonid M. Lytvynenko (IRA NASU), Prof. Ilya I. Zalyubovsky (KhNU), Prof. Michail F. Bondarenko, (KhNURE); **MSMW'13 Co-Organizers:** Dr. Alexei A. Kostenko (IRE NASU) and Prof. Alexander I. Nosich (IRE NASU)
TERATECH'13 Co-Chairs: Prof. Anatolii N. Pogorily (IMag of NASU and MESU) and Prof. Sergey I. Tarapov (IRE NASU)
MSMW'13 Local Organizing Chair: Dr. Alexei N. Kuleshov (IRE NASU)

Contact: MSMW'13, IRE NASU, 12, Ak. Proskury St., Kharkiv, 61085, Ukraine
Tel/Fax: +380 -57- 315- 2105; E-mail: msmw13@ire.kharkov.ua; http://www.ire.kharkov.ua/MSMW13/index.htm

Deadlines: Three-page camera-ready papers by March 30, 2013
Instructions at the MSMW'13 Website: http://www.ire.kharkov.ua/MSMW13/index.htm

AP-RASC' 13

2013 Asia-Pacific Radio Science Conference

Howard International House, Taipei, Taiwan, September 3-7, 2013

Call for Papers

Website: http://aprasc13.ntu.edu.tw

The "Asia-Pacific Radio Science Conference" (AP-RASC) is the Asia-Pacific regional URSI conference held between the URSI General Assemblies and Scientific Symposia. The objective of the AP-RASC is to review current research trends, present new discoveries, and make plans for future research and special projects in all areas of radio science, especially where international cooperation is desirable, and a particular emphasis is placed on promoting various research activities in the Asia-Pacific area.

Topics

- Electromagnetic Metrology
- Fields and Waves
- Radio Communication and Signal Processing Systems
- Electronics and Photonics
- Electromagnetic Environment and Interference
- Wave Propagation and Remote Sensing
- Ionospheric Radio and Propagation
- Waves in Plasmas
- Radio Astronomy
- Electromagnetics in Biology and Medicine

Young Scientist Programs

As in the URSI General Assemblies and Scientific Symposia, the following two programs are planned for young scientists:

- Student Paper Competition (SPC)
- Young Scientist Award (YSA)

Details on the Programs and the Application Guidelines are posted on the Conference website.

Special Issues

- AP-RASC'13 Special Issue will be published in "Radio Science".
- AP-RASC'13 Special Issue for Student Paper Competition will be published in "URSI Radio Science Bulletin".

Sponsored by

International Union of Radio Science (URSI)
National Taiwan University

In Cooperation with

National Science Council
Academia Sinica
Bureau of Foreign Trade, MOEA
The Institute of Electrical and Electronics Engineers, Inc.(IEEE)

Secretariat

E-mail: ctshih@tl.ntu.edu.tw
Tel: +886-2-23628136 Ext. 49
Fax: +886-2-23632090

Important Dates

Submission Deadline of One-Page Abstracts:
Feb. 28, 2013
Acceptance Notification:
April 30, 2013

Committees

Honorary Conference Chair
Phil Wilkinson, President of URSI, Australia

General Chair
Lou-Chuang Lee, National Central Univ., Taiwan

General Co-Chairs
Shyue-Ching Lu, Chunghwa Telecom. Co., Taiwan
Ruey-Beei Wu, National Taiwan Univ., Taiwan

International Advisory Committee
Co-Chairs:
Kazuya Kobayashi, Chuo Univ., Japan
Lou-Chuang Lee, National Central Univ., Taiwan

International Organizing Committee
Co-Chairs:
Lou-Chuang Lee, National Central Univ., Taiwan
Kazuya Kobayashi, Chuo Univ., Japan

Steering Committee
Chair:
Lou-Chuang Lee, National Central Univ., Taiwan

Organizing Committee
Co-Chairs:
Lou-Chuang Lee, National Central Univ., Taiwan
Shyue-Ching Lu, Chunghwa Telecom. Co., Taiwan
Ruey-Beei Wu, National Taiwan Univ., Taiwan

Technical Program Committee
Co-Chairs:
Hung-Chun Chang, National Taiwan Univ., Taiwan
Yen-Hsyang Chu, National Central Univ., Taiwan

Young Scientist Program Committee
Co-Chairs:
Yen-Hsyang Chu, National Central Univ., Taiwan
Ping-Cheng Yeh, National Taiwan Univ., Taiwan

Secretary
Tzong-Lin Wu, National Taiwan Univ., Taiwan

Information for authors

Content

The *Radio Science Bulletin* is published four times per year by the Radio Science Press on behalf of URSI, the International Union of Radio Science. The content of the *Bulletin* falls into three categories: peer-reviewed scientific papers, correspondence items (short technical notes, letters to the editor, reports on meetings, and reviews), and general and administrative information issued by the URSI Secretariat. Scientific papers may be invited (such as papers in the *Reviews of Radio Science* series, from the Commissions of URSI) or contributed. Papers may include original contributions, but should preferably also be of a sufficiently tutorial or review nature to be of interest to a wide range of radio scientists. The *Radio Science Bulletin* is indexed and abstracted by INSPEC.

Scientific papers are subjected to peer review. The content should be original and should not duplicate information or material that has been previously published (if use is made of previously published material, this must be identified to the Editor at the time of submission). Submission of a manuscript constitutes an implicit statement by the author(s) that it has not been submitted, accepted for publication, published, or copyrighted elsewhere, unless stated differently by the author(s) at time of submission. Accepted material will not be returned unless requested by the author(s) at time of submission.

Submissions

Material submitted for publication in the scientific section of the *Bulletin* should be addressed to the Editor, whereas administrative material is handled directly with the Secretariat. Submission in electronic format according to the instructions below is preferred. There are typically no page charges for contributions following the guidelines. No free reprints are provided.

Style and Format

There are no set limits on the length of papers, but they typically range from three to 15 published pages including figures. The official languages of URSI are French and English: contributions in either language are acceptable. No specific style for the manuscript is required as the final layout of the material is done by the URSI Secretariat. Manuscripts should generally be prepared in one column for printing on one side of the paper, with as little use of automatic formatting features of word processors as possible. A complete style guide for the *Reviews of Radio Science* can be downloaded from http://www.ips.gov.au/IPSHosted/NCRS/reviews/. The style instructions in this can be followed for all other *Bulletin* contributions, as well. The name, affiliation, address, telephone and fax numbers, and e-mail address for all authors must be included with

All papers accepted for publication are subject to editing to provide uniformity of style and clarity of language. The publication schedule does not usually permit providing galleys to the author.

Figure captions should be on a separate page in proper style; see the above guide or any issue for examples. All lettering on figures must be of sufficient size to be at least 9 pt in size after reduction to column width. Each illustration should be identified on the back or at the bottom of the sheet with the figure number and name of author(s). If possible, the figures should also be provided in electronic format. TIF is preferred, although other formats are possible as well: please contact the Editor. Electronic versions of figures *must* be of sufficient resolution to permit good quality in print. As a rough guideline, when sized to column width, line art should have a minimum resolution of 300 dpi; color photographs should have a minimum resolution of 150 dpi with a color depth of 24 bits. 72 dpi images intended for the Web are generally *not* acceptable. Contact the Editor for further information.

Electronic Submission

A version of Microsoft *Word* is the preferred format for submissions. Submissions in versions of T_EX can be accepted in some circumstances: please contact the Editor before submitting. *A paper copy of all electronic submissions must be mailed to the Editor, including originals of all figures.* Please do *not* include figures in the same file as the text of a contribution. Electronic files can be send to the Editor in three ways: (1) By sending a floppy diskette or CD-R; (2) By attachment to an e-mail message to the Editor (the maximum size for attachments *after* MIME encoding is about 7 MB); (3) By e-mailing the Editor instructions for downloading the material from an ftp site.

Review Process

The review process usually requires about three months. Authors may be asked to modify the manuscript if it is not accepted in its original form. The elapsed time between receipt of a manuscript and publication is usually less than twelve months.

Copyright

Submission of a contribution to the *Radio Science Bulletin* will be interpreted as assignment and release of copyright and any and all other rights to the Radio Science Press, acting as agent and trustee for URSI. Submission for publication implicitly indicates the author(s) agreement with such assignment, and certification that publication will not violate any other copyrights or other rights associated with the submitted material.

APPLICATION FOR AN URSI RADIOSCIENTIST

I have not attended the last URSI General Assembly, and I wish to remain/become an URSI Radioscientist in the 2012-2014 triennium. Subscription to *The Radio Science Bulletin* is included in the fee.

(please type or print in BLOCK LETTERS)

Name : Prof./Dr./Mr./Mrs./Ms. _____
Family Name First Name Middle Initials

Present job title: _____

Years of professional experience: _____

Professional affiliation: _____

I request that all information be sent to my ☐ home ☐ business address, i.e.:

Company name: _____

Department: _____

Street address: _____

City and postal/zip code: _____

Province/State: _____ Country: _____

Phone: _____ ext._____ Fax: _____

E-mail: _____

Areas of interest (Please tick)

☐ A Electromagnetic Metrology
☐ B Fields and Waves
☐ C Radio-Communication Systems & Signal Processing
☐ D Electronics and Photonics
☐ E Electromagnetic Environment & Interference
☐ F Wave Propagation & Remote Sensing
☐ G Ionospheric Radio and Propagation
☐ H Waves in Plasmas
☐ J Radio Astronomy
☐ K Electromagnetics in Biology & Medicine

I would like to order :

☐ An electronic version of the RSB downloadable from the URSI web site
(The URSI Board of Officers will consider waiving the fee if a case is made to them in writing.) 40 Euro

Method of payment : VISA / MASTERCARD (we do not accept cheques)

Credit card No ☐☐☐☐ ☐☐☐☐ ☐☐☐☐ ☐☐☐☐ Exp. date _____

CVC Code: _____ Date : _____ Signed _____

Please return this signed form to :

The URSI Secretariat
c/o Ghent University / INTEC
Sint-Pietersnieuwstraat 41
B-9000 GHENT, BELGIUM
fax (32) 9-264.42.88